

Structure-Activity Relationship Study of Antimicrobial Peptoids Against

Cryptococcus neoformans

By

Erin Yeatts

A Thesis Submitted in Partial Fulfillment of the Requirements for the Degree of Master
of Science in Chemistry

Middle Tennessee State University

December 2021

Thesis Committee:

Dr. Kevin Bicker, Chair

Dr. Mary Farone

Dr. Scott Handy

ABSTRACT

Cryptococcal meningitis, caused by the fungal pathogen *Cryptococcus neoformans*, is a devastating disease with a mortality rate of over 80 percent. While usually innocuous, other fungi such as *Candida albicans* can cause persistent infections such as urinary tract infections, oral thrush, sepsis and more. Because of the increasing prevalence of resistance to antifungals and the high mammalian toxicity of current treatments, the development of new antifungal therapies is vital. This research project utilized a structure-activity relationship (SAR) study of a previously discovered lead antifungal peptoid termed RMG8-8. This 3-round study focused on three main structural derivatives: the lipophilic tail, aliphatic side chains, and aromatic side chains. Round 1 compounds were tested against *C. albicans* and *C. neoformans*, while the other two rounds were tested against only *C. neoformans*, as early derivative testing showed poor activity against the former. Cytotoxicity testing was also performed on all derivatives against mammalian HepG2 cells, and select compounds were tested for hemolytic activity against human red blood cells. While no derivative was improved across all data points, there were improvements made to hemolytic activity with derivative EJY9. There are many candidates for further investigation generated from this research, including halogenated derivatives (EJY17), compounds with increased potency against *C. albicans* (EJY5 and EJY7), and compounds with chiral side chains (EJY16).

TABLE OF CONTENTS

Abstract	ii
Table of Contents	iii
List of Figures	vi
List of Tables	viii
Chapter One: Introduction	1
Pathogenic Fungi	1
Antifungals	3
Antimicrobial Resistance	4
Antimicrobial Peptides	5
Peptides vs. Peptoids	6
Antifungal Peptoids	8
Peptoid Design and Discovery: PLAD Assay	13
Discovery of Lead Compound: RMG8-8	14
SAR Studies	14
Thesis Statement: RMG8-8 SAR	15
Chapter Two: Experimental Methods	16
Materials	16

Synthesis of Mmt-protected Diamines	16
Synthesis of Boc-protected Diamines	17
General Peptoid Synthesis Procedure	17
EJY1 Synthesis	18
EJY2 and EJY5 Synthesis	18
Purification	20
MS Analysis	20
Minimum Inhibitory Concentration (MIC) Determination Against <i>Candida albicans</i>	20
Minimum Inhibitory Concentration (MIC) Determination Against <i>Cryptococcus neoformans</i>	21
Mammalian Cytotoxicity Assay	22
Hemolytic Assay	24
Chapter Three: Results and Discussion	26
SAR Overview	26
Round 1 Results	34
Round 2 Results	38
Round 3 Results	42

Hemolytic Activity	46
Chapter Four: Conclusions	48
References	49
Appendix	52

LIST OF FIGURES

Figure 1: Peptide vs. Peptoid	7
Figure 2: Peptoid Synthetic Scheme	9
Figure 3: Peptoid 1	10
Figure 4: Structure of AEC5	11
Figure 5: Structure of β -5	11
Figure 6: Structure of RMG8-8	12
Figure 7: Structure of Peptoid 17	13
Figure 8: RMG8-8 Structure	27
Figure 9: Round 1 Structures	29
Figure 10: Round 2 Structures	31
Figure 11: Round 3 Structures	33
Figure 12: Mass Spectra of EJY1	53
Figure 13: Mass Spectra of EJY2	54
Figure 14: Mass Spectra of EJY3	55
Figure 15: Mass Spectra of EJY4	56
Figure 16: Mass Spectra of EJY5	57
Figure 17: Mass Spectra of EJY6	58

Figure 18: Mass Spectra of EJY7	59
Figure 19: Mass Spectra of EJY8	60
Figure 20: Mass Spectra of EJY9	61
Figure 21: Mass Spectra of EJY10	62
Figure 22: Mass Spectra of EJY11	63
Figure 23: Mass Spectra of EJY12	64
Figure 24: Mass Spectra of EJY13	65
Figure 25: Mass Spectra of EJY14	66
Figure 26: Mass Spectra of EJY15	67
Figure 27: Mass Spectra of EJY16	68
Figure 28: Mass Spectra of EJY17	69
Figure 29: Mass Spectra of EJY18	70
Figure 30: Mass Spectra of EJY19	71
Figure 31: Mass Spectra of EJY20	72
Figure 32: Mass Spectra of EJY21	73
Figure 33: Mass Spectra of EJY22	74

LIST OF TABLES

Table 1: Round 1 Yields	34
Table 2: Round 1 Hydrophobicity Comparison	35
Table 3: Round 1 MIC and TD ₅₀ Data	38
Table 4: Round 2 Yields	39
Table 5: Round 2 Hydrophobicity Comparison	40
Table 6: Round 2 MIC and TD ₅₀ Data	41
Table 7: Round 3 Yields	43
Table 8: Round 3 Hydrophobicity Comparison	44
Table 9: Round 3 MIC and TD ₅₀ Data	45
Table 10: HC ₁₀ Values	47

CHAPTER ONE: INTRODUCTION

Pathogenic Fungi

Microorganisms such as fungi are ubiquitous in the environment. Some are innocuous while others have varying degrees of pathogenicity. *Candida albicans*, a yeast which is known for being a part of the normal human microbiome, is an opportunistic pathogen which may lead to infection in immunocompromised individuals or those who lack a robust commensal microbiome. Because of its prevalence, *C. albicans* frequently infiltrates healthcare environments and is one of the leading causes of hospital-acquired infections in the United States.¹ Central-line-associated bloodstream infections, catheter-associated urinary tract infections, and infections via prosthetic implants are some of the ways in which *C. albicans* can be perniciously introduced into the body and take its toll.^{1,2} Candidemia, which is the presence of a *Candida* infection in the bloodstream, has a mortality rate of approximately 30-60% depending on patient demographics, and *C. albicans* is the prominent species that causes these infections.³

One characteristic virulence factor of *C. albicans* is its ability to form biofilms when in unfavorable or threatening environments. A biofilm is a collection of adherent hyphae cells that form a thin film within the extracellular matrix. Biofilm formation can occur on abiotic surfaces such as implants and catheters, or on biological surfaces like oral mucosal cells.⁴ Biofilms are significantly more resistant to antimicrobial treatments and host immunity than budding yeast cells due to the impenetrable conglomeration that is formed. To make matters worse, bacteria present in the body can interact with established fungal biofilms and form multispecies biofilms which are even more difficult to treat.⁵ All

it takes is a “perfect storm” of conditions to turn a commensal fungus into a rampant untreatable infection.

Unlike *C. albicans*, *Cryptococcus neoformans* is a fungal pathogen that is not part of the normal microbiota in humans. *C. neoformans* is found in the environment such as in soil and water due to bird droppings. It can enter the body through respiration and cause a pulmonary infection called cryptococcosis in immunocompromised individuals. *C. neoformans* has a polysaccharide capsule which surrounds the cell membrane and contributes to its high virulence.⁶ The organism can shed large amounts of capsular material into the body which can spread to other susceptible areas such as the central nervous system.⁷ The capsule also helps the pathogen evade phagocytosis by immune cells more so than non-encapsulated organisms.⁷ Hence, the impact on an immunocompromised individual is even more severe. As *C. neoformans* infiltrates the central nervous system, an infection of the meninges called cryptococcal meningitis (CM) can occur.⁸

Cryptococcal meningitis affects almost one million people worldwide and causes several hundred thousand deaths per year.⁹ While CM is a worldwide disease, low-income and middle-income countries take the brunt of the impact.¹⁰ Human immunodeficiency virus (HIV) and acquired immunodeficiency syndrome (AIDS) are the most common precursors to cryptococcal infections, with around 15-20% of AIDS-related deaths being caused by cryptococcosis.^{10,11} Incidence of HIV/AIDS is significantly higher in Sub-Saharan Africa than any other part of the world.^{8,10} This, along with widespread poverty, leads to an overwhelming majority of cases presenting in this region.⁸ While the United States is far less impacted by cryptococcal meningitis, there are still thousands of hospitalizations resulting in hundreds of deaths caused by this infection.¹¹

Another infectious fungal culprit present in North America is *Cryptococcus gattii*, which can infect immunocompetent as well as immunosuppressed individuals. It was first recognized in British Columbia, Canada and made its way to the Pacific Northwest region of the United States with the first clinical isolation occurring in 2006.¹² Similarly to *C. neoformans*, *C. gattii* is introduced into the body through respiration and can infect the lungs, eventually leading to cryptococcoma lesions in the lungs and brain. It is now considered an endemic pathogen in the United States and it continues to warrant investigative priority as average mortality rates of these infections range from 20-33%.¹³

Antifungals

Because fungi are eukaryotes, agents that are active against fungal cells tend to be active against host cells as well.¹⁴ Antifungal agents such as fluconazole, flucytosine, and amphotericin B (AmB) are currently available to treat fungal infections caused by *C. albicans* and *C. neoformans*, and while these can be potent against fungal infections, they are known to have higher than ideal mammalian cytotoxicity.¹⁵ Up to 50% of recipients experience acute renal failure when treated with AmB.¹⁶ AmB is a polyene antifungal drug that forms pores in the membrane of fungal cells after binding to ergosterol, without which the cell cannot survive.¹⁷ Because of its high mammalian toxicity, it is only administered in cases of severe systemic infections such as cryptococcal meningitis.

Flucytosine is a base pyrimidine analog drug and interestingly, has no antifungal activity itself, but serves as a prodrug.¹⁸ Once it is taken up by the fungal cell, it is deaminated into 5-fluorouracil (5-FU), which does have antimycotic activity. Fungal cells that do not contain the deaminase hardware to modify flucytosine are not susceptible to

this drug. 5-FU cannot be directly administered as an antifungal treatment because it is extremely toxic to mammalian cells and has insufficient uptake by fungal cells.¹⁹ Even though flucytosine is characterized by gastrointestinal and hepatic toxicity, it is still one of the most effective, and therefore expensive, antifungals on the market. It is often used in conjunction with AmB for especially resistant infections.¹⁹

As the name suggests, fluconazole is in the azole class of antifungal agents. It works by interrupting the fungal ergosterol pathway by binding to cytochrome P450.¹⁸ While fluconazole is significantly less toxic than amphotericin B and flucytosine, it is not as effective for broad spectrum treatment and has up to a 20% relapse rate when used as a monotherapy.^{16,20} Because of this, it is most often administered after initial treatment with another more potent drug and does best as a maintenance or prophylactic therapy.¹⁵

Impoverished countries, which tend to be disproportionately affected by these fungal infections, have limited access to the more potent and costly antifungals like flucytosine.^{11,20} As a whole, treatment for infections like cryptococcal meningitis can be prolonged, leaving affected individuals at the mercy of maintenance therapy for several months to years.¹⁵ Quality of life is severely hindered for patients with these obstinate infections.

Antimicrobial Resistance

While no drug therapy is perfect, modern medicine has made great progress in contributing to the decrease in mortality caused by microbial infections. Even so, many pathogens have developed resistance to current treatments. Known as antimicrobial resistance (AMR), this phenomenon has put pressure on the medical community to

discover and create new therapies to combat these infectious agents. Pathogenic bacteria and fungi have developed mechanisms both transient and heritable that render antimicrobial therapies ineffective. One example of fluconazole resistance in *C. albicans* is due to a point mutation that is inherited by offspring. This variation occurs in the *ERG11* gene which changes drug-target interaction.²¹ Several other point mutations have been observed in *C. albicans*; however, their influence on drug resistance remains unclear.¹⁵

On the contrary, *C. neoformans* has displayed resistance to fluconazole with transient qualities. Studies have shown *C. neoformans* to be resistant when presented with high concentrations of fluconazole but becomes susceptible when the drug is removed. Known as hetero-resistance, this is thought to be caused by aneuploidy, which is a missing or extra chromosomes in the isolate. Hetero-resistance can be combatted with combination therapy of fluconazole and flucytosine, if available.²¹ Another resistance mechanism of *C. neoformans* happens when the cells first infect the lungs. They transform into large polyploid cells called titan cells. These titan cells possess thicker cell walls and tightly cross-linked capsules which help them evade phagocytic host cells.²¹ Interestingly, titan cells produce daughter cells that show enhanced resistance to fluconazole due to aneuploidy. Some *C. neoformans* strains that produce enlarged capsules have shown resistance to amphotericin B, and this is thought to be due to decreased drug penetration.²¹

Antimicrobial Peptides

The scientific community has extensively looked to naturally occurring compounds to emulate for the development of modern pharmaceuticals. One such group being antimicrobial peptides (AMPs). These omnipresent compounds were first discovered

almost 100 years ago by Alexander Fleming.²² Starting with the isolation of lysozyme and eventually leading to the discovery of thousands of antimicrobial compounds in plants, animals, insects, and even bacteria, these defensive structures have discreetly protected their hosts.²² Because these compounds are a part of the human body's innate immune system, they have low toxicity and continue to be widely studied by many. Most AMPs contain up to 50 amino acids with a wide variety of sequences. Generally, they are comprised of cationic residues as well as hydrophobic areas, creating an overall amphipathic structure.²² Because of the peptides' positive charge, they bind to the negatively charged membranes of microbes and work to eliminate pathogens through membrane disruption mechanisms such as pore formation, essentially leaking out the contents of the microbial cell.²³ AMPs present a solid foundation for the development of potential antimicrobial agents. However, they have their shortcomings which prevent them from having clinical applications. AMPs are quickly recognized and eliminated by degradative enzymes in the body, giving them a short *in vivo* half-life, averaging under an hour.^{24,25} This, as well as poor bioavailability, results in them being rendered useless before they can act against pathogenic cells in the body.

Peptides vs. Peptoids

The use of peptidomimetics is one way to overcome the inadequacies of AMPs. A slightly altered structure is enough to evade proteolytic degradation and increase bioavailability while maintaining a similar mode of action.²⁶ Stereochemical inversion is an approach which increases peptide stability by changing L-amino acids to D-amino acids, as proteolytic enzymes generally only recognize L-amino acid peptides.²⁷ Along the same

reasoning, side chain modification can introduce chirality which promotes more impactful and stable peptide secondary structure.²⁸ Another way to make use of peptidomimetics is through N-alkylation. One class of compounds called N-substituted glycines, or peptoids, utilizes this approach. Unlike peptides which exhibit side chains on the α -carbon of the amino acid building blocks, peptoids contain side chains on the nitrogen of the amide backbone, as shown in **Figure 1**. Because of their unique structure, peptoids are not recognized by proteases and have better *in vivo* stability than their peptide counterparts, while still maintaining low toxicity.²⁵⁻²⁹ They also exhibit increased hydrophobicity which aids in cell permeability and bioavailability.³⁰



Figure 1: Peptide vs. Peptoid. The difference in side chain position between peptides and peptoids.

Antifungal Peptoids

Antimicrobial peptoids have been gaining more awareness in the past 20 years, and their efficacy against a variety of microorganisms continues to be studied. They are relatively easy to synthesize as they employ the use of solid-phase synthesis on polystyrene resin with a Rink™ Amide linker. Through the submonomer approach first developed by Zuckermann in 1992, peptoids can be pieced together with alternating steps of acylation and amination.³¹ A schematic of this approach to peptoid synthesis is shown in **Figure 2**. The chemical linker on the solid-phase resin is usually Fmoc protected, so the first step in synthesis is to remove this group with the base piperidine. Bromoacetic acid (BrAcOH) is then added in conjunction with diisopropylcarbodiimide (DIC), which activates the carboxy group, allowing it to acylate the secondary amine exposed on the resin. The second step, amination, induces nucleophilic acyl substitution by displacing the bromide with an amine.³² Repetition of these steps introduces the side chain residues that make each peptoid structure unique.

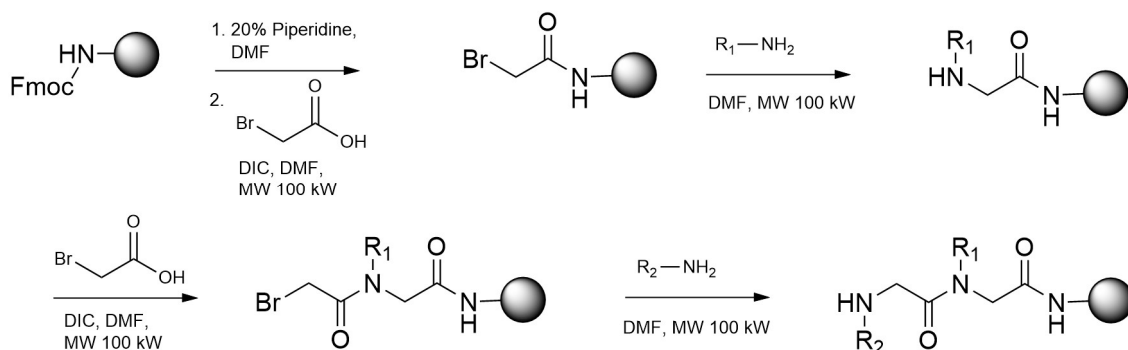


Figure 2: Peptoid Synthetic Scheme. Submonomer approach with alternating steps of acylation and amination.

The first reported structured and biologically active peptoid, termed Peptoid 1 (**Figure 3**), came from the Barron lab and was developed to mimic magainin-2, an α -helical AMP.³³ Peptoid 1 (**Figure 3**) and its analogs were systematically tested for potency against Gram-negative and Gram-positive bacteria and also for hemolytic activity. This report paved the way for further design and development of antimicrobial peptoids. While peptoids have been broadly tested for their activity against bacterial pathogens, their activity against fungal pathogens has just recently become an area of interest.

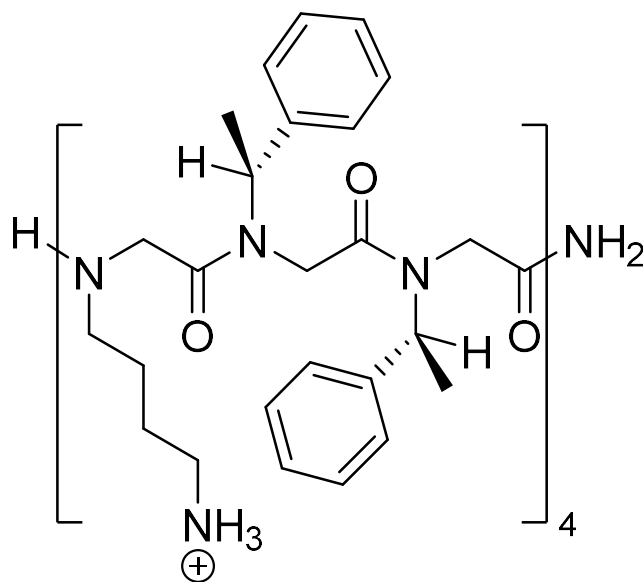


Figure 3: Peptoid 1. Structure of Peptoid 1, the first biologically active peptoid from the Barron lab.

The Bicker lab has identified multiple antifungal peptoids, including AEC5 (**Figure 4**), which showed noteworthy activity against *C. neoformans* with comparable potency to currently available antifungal therapies.³⁰ This compound was later modified to produce another notable peptoid called β -5 (**Figure 5**).³⁴ An additional compound discovered by the Bicker lab, RMG8-8, has recently yielded promising results against *C. neoformans* and will be elaborated on in subsequent sections (**Figure 6**).³⁵

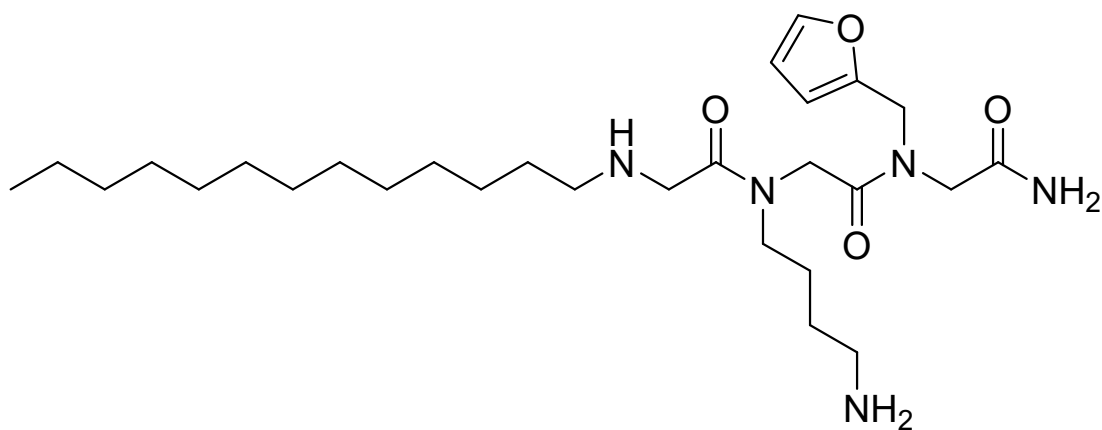


Figure 4: Structure of AEC5. One of the first antifungal peptoids discovered by the Bicker lab.

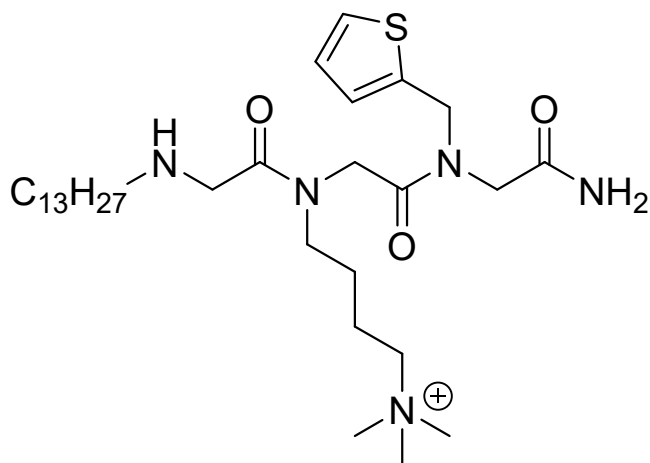


Figure 5: Structure of β -5. An improved derivative of AEC5.

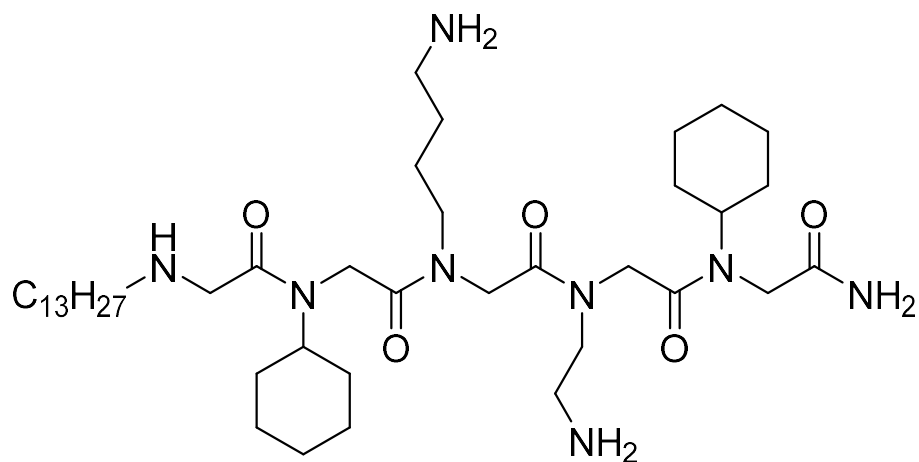


Figure 6: Structure of RMG8-8. Another peptoid with antifungal activity from the Bicker lab.

Other antifungal peptoids that have been reported include a compound called peptoid 17 discovered by research groups of Cobb and Lundy (**Figure 7**).^{36,37} This peptoid proved effective against *C. albicans* biofilms and cross-kingdom biofilms while sustaining low cytotoxicity.

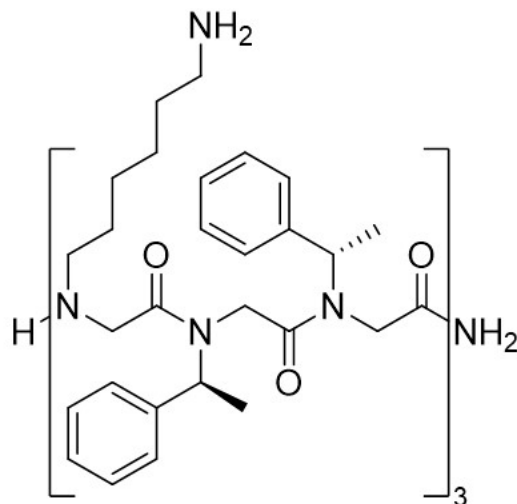


Figure 7: Structure of Peptoid 17. An antibiofilm peptoid coming from the Cobb and Lundy labs.

Peptoid Design and Discovery: PLAD Assay

Design, synthesis, and screening of potentially effective antimicrobial peptoids is a tedious endeavor, so combinatorial libraries and high-throughput screening methods are essential for quick identification. Recognizing a deficit, the Bicker lab developed an assay called the Peptoid Library Agar Diffusion (PLAD) assay which utilizes a branched system with a disulfide linker allowing for two identical peptoid sequences that can be orthogonally chemically cleaved.³⁸ After split-and-pool combinatorial library synthesis, the resin beads containing the two peptoid strands are plated in soft agar that has been inoculated with the fungi or bacteria of interest as well as a reducing agent. After agar

hardening and overnight incubation, the reducing agent cleaves the disulfide linked peptoid strand known as the beta-strand. The beta-strand is then free to act against the plated microorganism and zones of inhibition are easily examined. The beads with significant zones of inhibition can then be physically removed from the plate, and the remaining alpha-strand is cleaved and analyzed via tandem mass spectrometry to elucidate the peptoid sequence.³⁸ Bulk syntheses of promising compounds and their derivatives can then be achieved, and these peptoids can be studied further.

Discovery of Lead Compound: RMG8-8

One particular combinatorial library created by split-and-pool synthesis was developed by Dr. R. Madison Green and analyzed against *C. albicans* via the PLAD assay.³⁵ This led to the discovery of a compound with moderate activity against *C. albicans* termed RMG8-8. With a minimum inhibitory concentration (MIC) of 25 µg/mL and low mammalian cytotoxicity, RMG8-8 was selected to be characterized further. While not significantly active against *C. albicans*, this lead compound proved to have high activity against *C. neoformans* with an MIC of 1.56 µg/mL. Based on this data, it was decided that a structure-activity relationship (SAR) study of RMG8-8 would be a valuable project for the lab to complete.

SAR Studies

SAR studies utilize iterative design to modify structures and can be helpful in determining the pharmacological significance of each peptoid monomer. One method used to determine each position's role in overall function is called a sarcosine scan. Sarcosine

in peptoids is parallel to alanine in peptides. Each submonomer of a peptoid is replaced one at a time with a sarcosine. The effect of a single residue on the overall pharmacological activity of a compound can then be deduced. Such a technique was done with the tripeptoid AEC5.³⁴ It is widely accepted that cationic charge and hydrophobicity play an important role in a compound's efficacy.^{29,34} The proper balance between these characteristics must be achieved in order to develop a therapeutic compound worthy of clinical application. This was further verified with the AEC5 sarcosine scan and successive SAR study. The lipophilic tail, cationic amine, and aromatic heterocycle residues all played significant roles in the efficacy of AEC5. To further optimize this compound, methodical modification to each submonomer type was performed. The top performing derivative in each position was then carried on to the next round, resulting in a more optimal compound termed β -5.³⁴

Thesis Statement: RMG8-8 SAR

The ultimate goal of this project was to optimize the activity of a lead compound, RMG8-8, through an iterative SAR study against *C. neoformans*. We pursued this goal because antifungal resistance is widespread, and immunocompromised individuals are severely impacted by cryptococcal meningitis and other fungal infections with no nontoxic treatment options. To accomplish this goal, we designed a 3-round SAR study with each round focusing on a different submonomer type. All compounds were tested for potency and toxicity in order to classify the overall efficacy of each modification.

CHAPTER TWO: EXPERIMENTAL METHODS

Materials

All reagents were purchased at greater than 95% purity. Reagents and materials were purchased from Fisher Scientific (Waltham, MA), Alfa Aesar (Haverhill, MA), TCI America (Portland, OR), Amresco (Solon, OH), EMD Millipore (Billerica, MA), Supra Sciences (Belmont, CA), Corning (Tewksbury, MA) and Chem-Impex (Wood Dale, IL). Human red blood cells (hRBCs) were acquired from Innovative Research (Novi, MI).

Synthesis of Mmt-protected Diamines:

The desired diamine [1,2-diaminoethane (10.4 mL; 155 mmol) or 1,4-diaminobutane (15.8 mL; 155 mmol)], was added to dichloromethane (DCM; 30 mL) and stirred on ice for 10 minutes. Monomethoxytrityl chloride (Mmt, 5.25 g; 17 mmol) was dissolved into 100 mL of DCM and added dropwise over 1 hour using an addition funnel. The reaction was removed from ice and allowed to warm to room temperature and continued to stir for 4 hours. Solvent was removed *in vacuo* and remaining residue was dissolved in 1:1 0.5 M sodium bicarbonate (NaHCO₃):DCM (60 mL). Extraction was performed twice, and organic layers were combined and dried with calcium chloride. Solvent was removed *in vacuo*, and compound presence was confirmed with MS. Yields of Mmt-diaminoethane and Mmt-diaminobutane were 7.058 g (21 mmol) and 7.962 g (22 mmol) respectively. Yields indicate an impure product as the percent yield for each Mmt-diamine was greater than 100. The likely remaining impurity was residual diamine. Mmt-protected diamines were used successfully without further purification.

Synthesis of Boc-protected Diamines:

Methanol (60 mL) and hydrochloric acid (HCl, 3.82 mL; 136 mmol) were combined and stirred on ice for 15 minutes. Boc-anhydride (16 mL; 70 mmol) and methanol (80 mL) were combined and cooled on ice for 30 minutes. The desired diamine [diaminoethane (3.062 mL; 46 mmol) or diaminobutane (4.6 mL; 46 mmol)] was added to the methanol/HCl solution and stirred on ice for 15 minutes. Deionized water (10 mL) was added to the amine solution and stirred for 30 minutes. The chilled Boc-anhydride solution was added dropwise to the amine solution while continuing to stir on ice. The solution was removed from ice and allowed to come to room temperature while stirring for 1 hour. The solvent was removed *in vacuo* and 1 M sodium hydroxide (NaOH; 30 mL) was added. Extraction was performed with DCM (30 mL) 2x and then brine 2x. The organic layer was dried with calcium chloride, solvent was evaporated *in vacuo*, and compound presence was confirmed with MS. Yields for Boc-diaminoethane and Boc-diaminobutane were 3.740 g (23 mmol, 50% yield) and 8.764 g (47 mmol, 102% yield) respectively. Yield of over 100% indicates possible impurities or error in calculations.

General Peptoid Synthesis Procedure:

Peptoids were synthesized on the solid phase using the submonomer approach as previously described.³¹ These methods were sufficient for synthesizing most of the peptoids studied here. More unique methods required for certain peptoids are described below. Polystyrene resin with a Rink Amide linker (loading capacity: 0.75 mmol/g) was placed in a fritted column and swelled with dimethylformamide (DMF) for 30 minutes followed by Fmoc deprotection with 20% piperidine 2x for 10 minutes each. A Kaiser test

was utilized to determine full Fmoc deprotection. After a DMF wash 3x, the resin was acylated with 2 M bromoacetic acid in anhydrous DMF (1.5 mL) and 3.2 M diisopropylcarbodiimide (DIC) in anhydrous DMF (1.5 mL). The reaction was microwaved at 10% power for 15 seconds 2x and then allowed to rock for 15 minutes. The solution was aspirated from the resin, and the resin was washed 3x with DMF. A Kaiser test was performed to ensure the reaction was successful. For submonomer addition, a 2 M solution of the desired amine (3 mL) was added to the resin and microwaved at 10% power for 15 seconds 2x and then placed on the rocker for 30 minutes. These alternating steps of acylation and amination were repeated with the necessary amines until the desired peptoid structure was achieved. Final submonomer addition for the lipophilic tail was allowed to rock overnight at 35°C to maintain amine solubility and improve reaction yield. Resin was washed with DMF 3x and DCM 3x and allowed to dry under vacuum for 5 minutes. To cleave the compound from the resin, a mixture of 95% trifluoroacetic acid (TFA): 2.5% triisopropylsilane (TIS): 2.5% H₂O was added and rocked for 1 hour. The reaction solution was drained from the resin into a 50 mL conical tube, and the TFA was evaporated under a stream of air. The resulting oil was reconstituted in 1:1 acetonitrile (ACN):H₂O (8 mL) in preparation for purification.

EJY1 Synthesis:

Synthesis for EJY1 followed that of the General Peptoid Synthesis Procedure until after the addition of the lipophilic tail. Following this addition, Boc protection of the N-terminal amine was achieved by treating with Boc-anhydride (430 μ L; 1.87 mmol) in 5% N-methylmorpholine (NMM) in DMF (5 mL) for 1 hour with rocking. The resin was

washed with DMF 3x and DCM 3x. To remove the Mmt protecting groups, the resin was treated 6x with 1% TFA in DCM (5 mL) for 10 minutes each, followed by washing with DCM 3x and DMF 3x. Resin amines were free based by treating with 5% NMM in DMF for 5 minutes and then trimethylated with methyl iodide (118 μ L; 1.9 mmol) and cesium carbonate (619 mg; 1.9 mmol) in DMF (5 mL) while rocking overnight at 25°C. Resin was washed with DMF 3x, water 3x, DMF 3x, then DCM 3x. The compound cleavage procedure was followed which also removed the N-terminal Boc group.

EJY2 and EJY5 Synthesis:

Synthesis for EJY2 and EJY5 followed that of the General Peptoid Synthesis Procedure until the addition of the aliphatic tail, which for these peptoids was a fatty acid. Fmoc-glycine-OH (222.75 mg; 0.75 mmol) was activated with 3-[Bis(dimethylamino)methyl]imidazolium hexafluorophosphate (HBTU, 284.4 mg; 0.75 mmol) in 5% NMM in DMF (7 mL) for 10 minutes. This solution was added to the resin and rocked for 1 hour. After aspiration and washing with DMF 3x, a Kaiser test was performed to verify successful coupling. 20% piperidine in DMF was used to remove Fmoc protecting groups (~ 7 mL 2x for 10 minutes each). Another Kaiser test was performed to confirm the removal of Fmoc. 4 molar equivalents of myristic acid (EJY2) and palmitic acid (EJY5) were activated with HBTU (284.4 mg; 0.75 mmol) in 5% NMM in DMF for 10 minutes. This solution was added to the resin and rocked for 1 hour. After aspiration, a DMF wash was performed 3x, and a Kaiser test was used to confirm proper coupling. The resin was then washed with DCM 3x and allowed to dry for 5 minutes under vacuum. The compound cleavage procedure was then followed.

Purification:

Peptoids were purified via Reversed-Phase High-Performance Liquid Chromatography (RP-HPLC) using a Varian Prepstar SD-1. A gradient of 0-100% water to acetonitrile containing 0.05% TFA made up the mobile phase, and a Supelco Ascentis C18 column (5 μ m; 25 cm x 21.2 mm; Sigma-Aldrich 581347-U) was used as the stationary phase. Peaks in the chromatogram above 0.1 AU were collected and analyzed via mass spectrometry. The peak product with the desired peptoid was dried down *in vacuo* and lyophilized overnight. Peptoids were then reconstituted in sterile 18 m Ω deionized water to create compound stocks of 20 mg/mL.

MS Analysis:

Rapid analysis of peptoids during synthesis was done using a “quick cleave” procedure. Quick cleaves of all compounds were performed by removing a small amount of resin from the synthesis sample and rocking with 500 μ L of TFA for 30 minutes. The TFA was evaporated under a stream of air and 1:1 ACN:H₂O (1 mL) was added. Samples were analyzed with electrospray ionization time-of-flight mass spectrometry (ESI-TOF MS) via Waters Synapt HDMS. For analysis of RP-HPLC purified products, the collected peaks were directly injected into the mass spectrometer and presence of the compounds’ mass/charge was verified (**Appendix**).

Minimum Inhibitory Concentration (MIC) Determination Against *Candida albicans*:

Antifungal minimum inhibitory concentration (MIC) assays were done following CLSI guidelines as previously described.^{30,39} Yeast extract peptone dextrose (YPD) agar

plates were streaked with *C. albicans* frozen culture stock and incubated for 24-48 hours at 35°C. After incubation, a sterile loop was used to transfer 1-2 colonies to 0.85% saline (5 mL). After vortexing for 30 seconds, the optical density at 600 nm was determined by a spectrophotometer and adjusted to the desired range of 0.15-0.25 if necessary. The addition of 0.1 mL cell solution to RPMI-MOPS (9.9 mL) produced a 1:100 cell solution. After vortexing, 0.5 mL of the 1:100 solution was added to 9.5 mL RPMI-MOPS to produce a 1:20 cell solution. 198 µL of the 1:20 solution was added to the wells of an opaque 96-well plate, apart from the wells designated for the medial control. Compound stocks of 20 mg/mL were used to prepare 2-fold serial dilutions, and 2 µL of each compound dilution were plated in triplicate as assigned on the plate map, giving final concentrations of 200, 100, 50, 25, 12.5, 6.25, and 3.13 µg/mL. Amphotericin B was used as a positive control, and sterile water was used for the vehicle control. The plates were incubated for 24 hours at 35°C.

After incubation, 20 µL of PrestoBlue was added to each well and incubated for 1 hour at 35°C. A SpectroMax M5 Plate Reader was used to determine fluorescence of each well with excitation at 555 nm and emission at 585 nm. MIC is the lowest compound concentration resulting in greater than 90% inhibition of microbial growth. This MIC study was performed in biological triplicate.

Minimum Inhibitory Concentration (MIC) Determination Against *Cryptococcus neoformans*:

MIC assays against *C. neoformans* were done similarly to the assay described above for *C. albicans* but with longer incubation times. YPD agar plates were streaked with *C.*

neoformans frozen culture stock and incubated for 72 hours at 35°C. After incubation, a sterile loop was used to transfer 1-2 colonies to 5 mL of 0.85% saline. After vortexing for 30 seconds, the optical density at 600 nm was determined by a spectrophotometer with the desired range of 0.15-0.25. The addition of 0.1 mL cell solution to 9.9 mL of RPMI-MOPS produced a 1:100 cell solution. After vortexing, 0.5 mL of the 1:100 solution was added to 9.5 mL RPMI-MOPS to produce a 1:20 cell solution. 198 µL of the 1:20 solution was added to the wells of an opaque 96-well plate, apart from the wells designated for the medial control. Compound stocks of 20 mg/mL were used to prepare 2-fold serial dilutions, and 2 µL of each compound dilution were plated in triplicate as assigned on the plate map, giving final concentrations of 200, 100, 50, 25, 12.5, 6.25, 3.13, and 1.56 µg/mL. Amphotericin B was used as a positive control, and sterile water was used for the vehicle control. The plates were incubated for 72 hours at 35°C.

After incubation, 20 µL of presto blue was added to each well and incubated for 8 hours at 35°C. A SpectroMax M5 Plate Reader was used to determine fluorescence of each well with excitation at 555 nm and emission at 585 nm. For the sake of time, it was determined that a manual read could be used to accurately determine MIC for each compound. This was done by visually verifying fungal growth vs no growth in the wells. This MIC study was performed in triplicate.

Mammalian Cytotoxicity Assay:

Cytotoxicity against HepG2 hepatocellular carcinoma cells was done as previously described. HepG2 cells were maintained in culture in T-75 flasks using Dulbecco's Modified Eagle's Media (DMEM) with phenol red pH indicator and supplemented with

10% fetal bovine serum (FBS) and 1% penicillin, streptomycin, and glutamine (PSG). The cells were incubated at 37°C and 5% CO₂ in a humidified incubator until desired confluency was achieved. The media was removed from the flask, and the cells were washed 1x with 10 mL of phosphate-buffered saline (PBS; 11.8 mM phosphate, 140.4 mM NaCl; pH 7.4) which was then discarded. To remove the adhered cells from the flask, 2 mL of trypsin was added, and the cells were incubated for 10 minutes. To quench the trypsin, 8 mL of phenol red-free DMEM with 10% FBS and 1% PGS was added, and the cell solution was transferred to a 15 mL conical tube. After the cells were pelleted by centrifugation at 1000 rpm for 5 minutes, the supernatant was poured off and cells resuspended in the volume of phenol red-free media needed for the assay. Cell concentration was determined by counting with a hemocytometer, and the solution was diluted with media until a concentration of 1x10⁵ cells/mL was achieved. A 100 µL aliquot of cell solution was added to each well of a 96-well plate, apart from the 3 wells used for a media control. Cells were incubated for 2-3 hours at 37°C and 5% CO₂ until cells were adherent.

Compound stocks of 20 mg/mL were used to prepare 2-fold serial dilutions of each compound in sterile water, giving final concentrations of 200, 100, 50, 25, 12.5, 6.25, 3.13 and 1.56 µg/mL. 11.1 µL of prepared compound solutions was added to the appropriate wells in triplicate as indicated on the plate map. A negative vehicle control of sterile water, as well as the aforementioned media control, were used. The plates were incubated for 72 hours at 37°C and 5% CO₂.

After incubation, 20 µL of 5 mg/mL 3-(4,5-Dimethylthiazol-2-yl)-2,5-Diphenyltetrazolium Bromide (MTT) in water was added to each well. The plate was

incubated for 3 hours at 37°C and 5% CO₂. Media was removed from each well using a sterile glass Pasteur pipette. 100 µL of DMSO was added to each well and incubated for 15 minutes at 37°C. Absorbance was read at 570 nm using a SpectroMax M5 Plate Reader. This MTT assay was performed in biological duplicate unless discrepant results were observed. If this was the case, the assay was performed in biological triplicate for further verification. The reported value is the average of biological replicates with standard deviation.

Hemolytic Assay:

Selected peptoids were prepared in 2-fold serial dilutions in PBS at the desired concentrations. Human red blood cells (hRBCs, 9 mL) were centrifuged at 1000 rpm for 10 minutes, and the supernatant was removed and discarded. A 10 mL aliquot of PBS was used to resuspend the hRBCs which were centrifuged again at 1000 rpm for 10 minutes. This PBS wash was completed two more times for a total of three washes. A 9 mL aliquot of PBS was added to the hRBCs, and 100 µL of cell solution was added to individual wells of a 96-well plate. Peptoid solutions (11.1 µL) were added to the appropriate wells in triplicate. A vehicle control of PBS and positive control of 1% Triton X-100 were added to wells in triplicate.

The plate was incubated at 37°C for 1 hour and centrifuged at 1000 rpm for 10 minutes. For each well, 5 µL of supernatant was transferred to 95 µL of PBS in a new 96-well plate. The absorbance at 405 nm was measured using a SpectraMax M5 Plate Reader, and the percent hemolysis was calculated as follows:

$$\% \text{ hemolysis} = \frac{(\text{OD}_{405\text{nm}} \text{ sample} - \text{OD}_{405\text{nm}} \text{ neg. control})}{(\text{OD}_{405\text{nm}} \text{ pos. control} - \text{OD}_{405\text{nm}} \text{ neg. control})} \times 100$$

This hemolytic assay was performed in triplicate.

CHAPTER THREE: RESULTS AND DISCUSSION

SAR Overview

RMG8-8 derivatives were synthesized via solid-phase synthesis on a polystyrene Rink Amide resin. Peptoid residues were added through the submonomer approach. The structure of RMG8-8 is shown in **Figure 8**. To measure compound potency, minimum inhibitory concentration (MIC) assays were performed. Round 1 was tested against *C. neoformans* as well as *C. albicans*, while Rounds 2 and 3 were tested against *C. neoformans* only because RMG8-8 and the early derivatives did not show good efficacy against *C. albicans*. Mammalian cytotoxicity was evaluated through a cell metabolic activity assay with HepG2 liver carcinoma cells, and selected compounds were tested for hemolytic activity against human red blood cells.

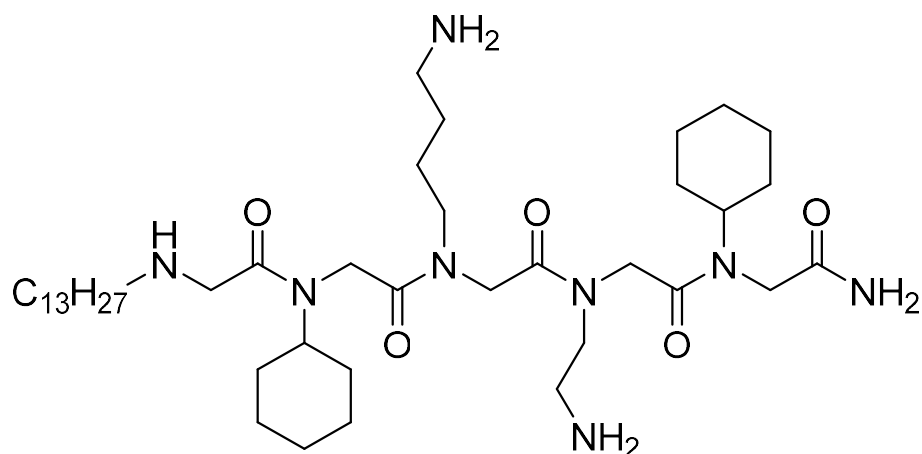


Figure 8: RMG8-8 Structure. RMG8-8 is a 5-mer consisting of cyclohexylamine residues in positions 1 and 4, *Nae* and *MLys* residues in positions 2 and 3, respectively, and a tridecylamine tail in the 5th position.

Round 1 of the SAR included modifications to the lipophilic tail in position 5, as well as miscellaneous alterations that did not belong in the other two rounds (**Figure 9**). The first derivatization of RMG8-8 was the trimethylation of the side chain amines (EJY1). This was done to lock in the cationic charge which we hypothesized would decrease the toxicity of the compound, consistent with a previous peptoid SAR.³⁴ Another derivative in Round 1 consisted of lengthening the *Nae* residue in position 2 to an *MLys* (EJY6) which was justified by a previous SAR study of compound AEC5.³⁴ In this study, a lysine derivative submonomer was less toxic than an *Nae* submonomer. Additionally, inverting positions 1 and 4 with 2 and 3 was done to determine if submonomer order would change the activity in any way (EJY7). Derivatives EJY2, EJY3, EJY4, and EJY5 all contained different tail variations: myristic acid, dihexylamine, dioctylamine, and palmitic acid, respectively. The fatty acids derivatives were chosen to determine if the toxicity would

decrease because these compounds are naturally occurring and early studies demonstrated that lipopeptoids with fatty acid tails were less toxic than those with aliphatic amine tails.²⁴ The double tails in EJY3 and EJY4 were hypothesized to increase potency as they would cover more area than a single tail and could potentially cause more fungal cell membrane disruption.

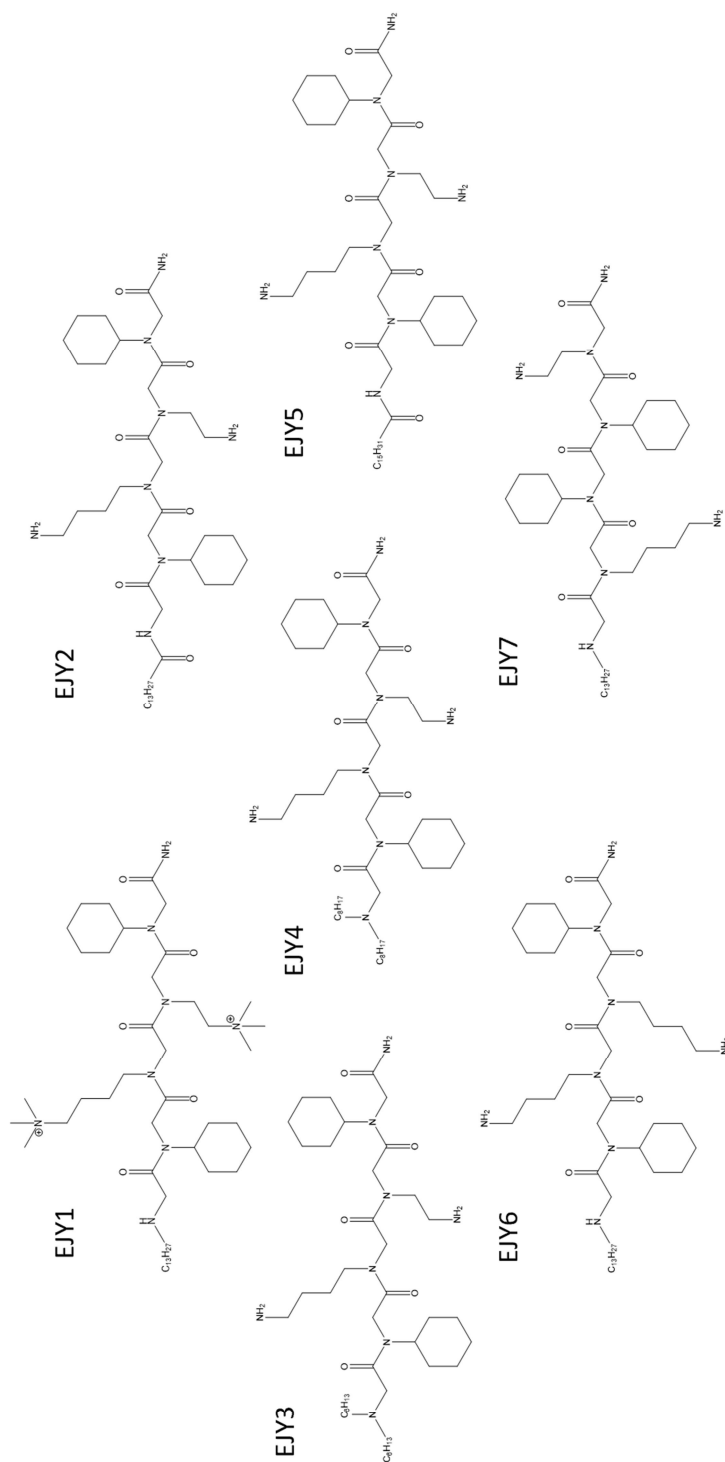


Figure 9: Round 1 Structures. Position 5 tail modifications and miscellaneous derivatives.

Round 2 consisted of aliphatic derivatives in positions 1 and 4 (**Figure 10**). These were chosen for multiple reasons including comparisons of size, cyclic versus straight chain alkanes, and heterocyclic effects. The amines tested were isopropylamine (EJY8), isobutylamine (EJY9), hexylamine (EJY10), cyclopentylamine (EJY11), cyclohexylmethylamine (EJY12), and tetrahydrofurfurylamine (EJY13).

Round 3 was the largest round, with nine compounds consisting of aromatic derivatives in positions 1 and 4 (**Figure 11**). The amines tested were aniline (EJY14), benzylamine (EJY15), L-alpha-methylbenzylamine (EJY16), 4-fluorobenzylamine (EJY17), naphthylamine (EJY18), 5-aminoindan (EJY19), tryptamine (EJY20), furfurylamine (EJY21), and 2-thiophenemethylamine (EJY22). *N*spe submonomers were utilized in EJY16 to observe how stereochemistry affects compound efficacy. Other modifications of note are the fluorinated benzene residues (EJY17) as halogenation has previously shown to have effect on activity,⁴⁰ and the aromatic heterocycles (EJY21, EJY22) as use of these impacted compound efficacy in a previous SAR study.³⁴

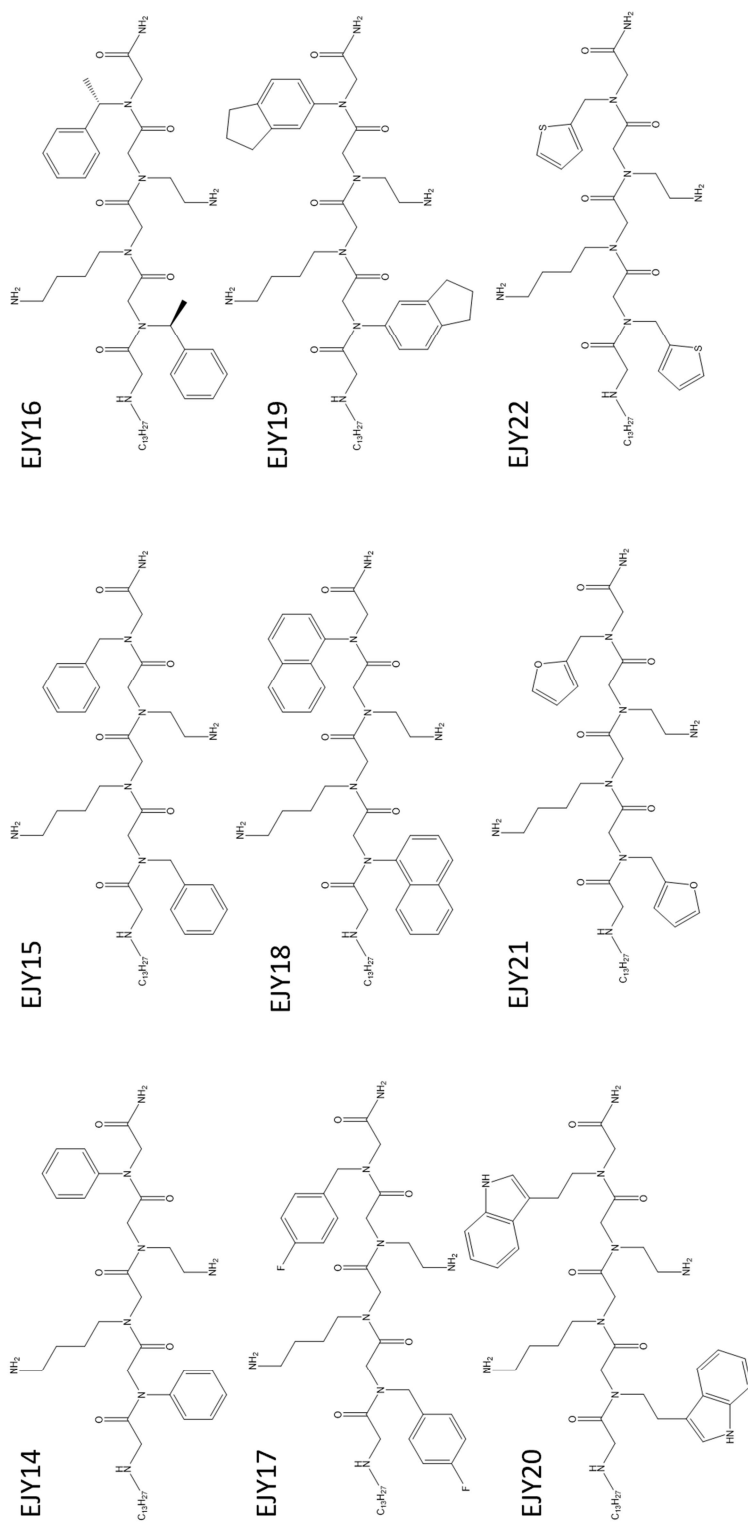


Figure 11: Round 3 Structures. Positions 1 and 4 modifications with aromatics.

Round 1 Results

Each compound was synthesized and purified as described, and yields were calculated to range between 0.75-58.7%, as seen in **Table 1**. Compound identity and molecular weights were confirmed with ESI-TOF MS (**Appendix**).

Compound	Expected MW (g/mol)	Observed MW (g/mol)	Yield (mg)	Percent Yield
EJY1	849	424*	1.2/10.7	0.75/6.7%
EJY2	792	792/396*	5.0	3.4%
EJY3	750	750/375*	33.6	23.8%
EJY4	806	806/403*	13.1	8.7%
EJY5	820	1640**/820/410*	52.9	34.4%
EJY6	792	1584**/792/396*	87.5	58.7%
EJY7	764	1528**/764/382*	40.1	28.0%

*m/2 value ** m·2 value

Table 1: Round 1 Yields. Compound yields and observed MW.

Trimethylation of the side chain amines in EJY1 proved particularly challenging as synthetic yields were clearly diminished in comparison to most of the other compounds. This warranted a second round of synthesis, hence the two yields provided. Generally, peptoid synthesis produces low yields, and high yield was not the concern of this research. However, current efforts are being made in the Bicker lab to increase synthetic yields.

Increased hydrophobicity is a characteristic which has been attributed to increased compound activity against microbe membranes. While this is a desired outcome, increased

hydrophobicity has also been associated with an increase in mammalian toxicity. A comparison of expected versus experimental hydrophobicities was made for each compound as shown in **Table 2**. The expected value is represented by the $cLogD_{7.4}$ calculated by a program called MarvinSketch. The $cLogD_{7.4}$ is the water:octanol distribution coefficient at biological pH 7.4 which denotes the hydrophobicity or hydrophilicity of a compound. The more negative the value, the more hydrophilic the compound. Inversely, the higher the value, the more hydrophobic. The experimental values are the percentage of acetonitrile (ACN) in water at which the compound eluted during HPLC purification. The higher the % ACN, the greater the hydrophobicity.

Compound	$cLogD_{7.4}$	Experimental % ACN
EJY1	-5.22	57.3
EJY2	-1.34	61.5
EJY3	-2.53	51.6
EJY4	-0.75	55.5
EJY5	-0.45	64.1
EJY6	-2.74	55.3
EJY7	-2.38	55.4

Table 2: Round 1 Hydrophobicity Comparison. Expected versus experimental hydrophobicities.

For the most part, these values trended in parallel. However, the expected hydrophobicity for EJY1 was much lower than was experimentally determined by ACN percentage. This can be explained by the relative pH for each of these values. MarvinSketch calculates *cLogD* at pH 7.4, in which the peptoid side chain amines would be in an equilibrium state between a cationic charge and neutral. However, EJY1 has a locked in cationic charge due to trimethylation of the side chain amines, so the *cLogD*_{7.4} is very negative when calculated. In the experimental % ACN EJY1 appears to be just as hydrophobic, if not more, as the other compounds. This is due to the pH of the mobile phase during HPLC being around pH 2 because of the 0.05% TFA that is added to the mobile phase. This lower pH induces all the peptoids' side chain amines to be predominantly in the cationic state, which would make them no different from EJY1 during HPLC purification, even though they would be different at biological pH.

First up for biological testing was to determine potency via the MICs against *C. albicans* and *C. neoformans* (**Table 3**). MIC is the concentration of compound required to inhibit 90% of fungal growth. Some values of note are the *C. albicans* MICs of EJY2 and EJY5 in comparison to RMG8-8. These derivatives displayed a 2-fold and 4-fold decrease in MIC compared to RMG8-8, respectively. This is interesting because both derivatives implemented the fatty acid tail. These same compounds against *C. neoformans* did not supersede the potency of RMG8-8 and its tridecylamine tail. EJY3, which contained the dihexylamine tail, showed poor activity against both fungi. EJY7, which consisted of swapping monomers in positions 1 and 4 with 2 and 3 displayed similar activity against *C. neoformans*, however, showed a 2-fold decrease in MIC against *C. albicans*. It is interesting to note that monomer order could potentially affect activity, as this has not yet

been thoroughly investigated with the Bicker lab lead compounds. EJY1 with the trimethylated amine side chains did not show any activity against *C. albicans* and did not surpass the activity of RMG8-8 against *C. neoformans*.

Mammalian cytotoxicity is an important factor to consider when developing new antifungal agents. It is critical that the treatment does not do more harm than good. For this SAR study, cytotoxicity was determined with a cell viability assay using HepG2 cells. This *in vitro* method is used to mimic the effects of compounds on the liver, as most molecules are metabolized by the liver.⁴¹ The TD₅₀, or the dose required to kill 50% of cells, of RMG8-8 was 175 µg/mL. Derivatives EJY1, EJY2, EJY3, EJY4, and EJY6 displayed either lower or similar toxicity to the lead compound. EJY5 displayed a significant increase in toxicity. The two extra carbons in the palmitic acid tail derivative had significant impact on the overall toxicity, as the myristic acid derivative (EJY2) displayed very low toxicity at 200 µg/mL.

A selectivity ratio (SR) can be calculated by dividing toxicity (TD₅₀) by potency (MIC) and is used to compare the potency and toxicity to get a picture of the overall efficacy of a compound. The greater the SR, the more selective the compound. In Round 1, the only derivative with a comparable *C. neoformans* SR to RMG8-8 was EJY6, which contained the extended amine chain (NLys) in position 2. Overall, it was determined that no tail derivative in Round 1 showed improvement over the tridecylamine tail of RMG8-8. While, as expected, EJY1 had lower toxicity than RMG8-8, its potency was not ideal for either fungal pathogen. The other derivatives either lacked the potency or were too toxic to beat the standard set by RMG8-8.

Compound	<i>cLogD</i> _{7.4}	<i>C. albicans</i> MIC (µg/mL)	<i>C. neoformans</i> MIC (µg/mL)	HepG2 TD ₅₀ (µg/mL)	Selectivity Ratio (<i>C. neoformans</i>)
RMG8-8	-2.38	25	1.56-3.13	175	56
EJY1	-5.22	200	12.5	>200	16
EJY2	-1.34	12.5	6.25	>200	32
EJY3	-2.53	>200	100	>200	2
EJY4	-0.75	25	6.25	162 ± 11	26
EJY5	-0.45	6.25	3.13	85 ± 0	27
EJY6	-2.74	25	3.13	165 ± 16	53
EJY7	-2.38	12.5	3.13	105 ± 0	34

Table 3: Round 1 MIC and TD₅₀ Data. A comparison of efficacy with RMG8-8.

Round 2

Since it was confirmed that the tridecylamine tail in position 5 was the optimal option, this was carried over to all derivatives in Round 2. As stated previously, Round 2 utilized aliphatic derivatives in positions 1 and 4. **Table 4** shows the yields and molecular weights that were determined after compound synthesis and purification. Yields ranged from 5.9-23.0%. Overall, Round 2 compounds proved to be more synthetically challenging than the previous round. This could be due to the fact that some of the aliphatic derivatives were bulkier than Round 1 derivatives which could increase steric hinderance.

Compound	Expected MW (g/mol)	Observed MW (g/mol)	Yield (mg)	Percent Yield
EJY8	684	684/342*	29.5	23.0%
EJY9	712	712/356*	7.9	5.9%
EJY10	768	768/384*	11.0	7.6%
EJY11	736	736/368*	10.9	7.9%
EJY12	792	792/396*	14.8	9.9%
EJY13	768	768/384*	12.9	9.0%

*m/2 value

Table 4: Round 2 Yields. Compound yields and observed MW.

As was done with Round 1, hydrophobicities were determined computationally and experimentally for Round 2 (**Table 5**). These two values trended comparably for each compound, and there were no glaring outliers. As expected, EJY8 and EJY13 displayed the lowest hydrophobicity as the isopropyl and tetrahydrofuran moieties of each compound reduce the number of methylenes and add a heteroatom, respectively. EJY10 with the straight-chain hexane residues was expected to be the most hydrophobic, and this was the case experimentally as well.

Compound	<i>cLogD</i> _{7.4}	Experimental % ACN
EJY8	-4.43	53.3
EJY9	-3.49	54.5
EJY10	-1.55	58.6
EJY11	-3.27	54.5
EJY12	-1.75	57.1
EJY13	-5.14	53.9

Table 5: Round 2 Hydrophobicity Comparison. Expected versus experimental hydrophobicities.

All Round 2 compounds were tested for their activity against *C. neoformans* using the previously described MIC assay. After potency testing, toxicity testing was completed for Round 2 against HepG2 cells. These results as well as the calculated SR values are shown in **Table 6**.

Compound	<i>cLogD</i> _{7.4}	<i>C. neoformans</i> MIC (µg/mL)	HepG2 TD ₅₀ (µg/mL)	Selectivity Ratio
RMG8-8	-2.38	1.56-3.13	175	56
EJY8	-4.43	25	>200	8
EJY9	-3.49	3.13	167 ± 9	53
EJY10	-1.55	1.56-3.13	61 ± 9	19
EJY11	-3.27	6.25	>200	32
EJY12	-1.75	1.56-3.13	62 ± 9	20
EJY13	-5.14	12.5-25	>200	8

Table 6: Round 2 MIC and TD₅₀ Data. Efficacy of Round 2 derivatives compared to RMG8-8.

EJY9 with the isobutyl monomers had only diminished antifungal activity and had the best efficacy of Round 2 derivatives, however, this compound still fell just short of RMG8-8. With the decreased hydrophobicity, EJY8 and EJY13 displayed the expected very low toxicity, but their SR values were pulled down by less than ideal MICs of 25 µg/mL.

It is important to note that the addition of a methylene group in EJY9 versus EJY8 modified biological activity. This was also the case for RMG8-8 and EJY12, which only differ by one methylene group as well. EJY12 is much more toxic than RMG8-8 but maintains potency. Likewise, EJY10 maintained the MIC of RMG8-8, but was significantly more toxic, resulting in a poor SR value. Ultimately, no Round 2 derivative could outrank RMG8-8, and therefore Round 3 continued as planned with the aromatic derivatives.

Round 3

As mentioned, Round 3 compounds had various aromatic moieties in positions 1 and 4. **Table 7** shows the synthesis yields and molecular weights of each compound. Similar to previous rounds, Round 3 structures were relatively challenging to synthesize. This is to be expected with the addition of bulky aromatic residues. However, sufficient yields were achieved to continue with the biological assays, and backup stock remains for each peptoid if further testing should ever be required.

Compound	Expected MW (g/mol)	Observed MW (g/mol)	Yield (mg)	Percent Yield
EJY14	752	751.3/376.2*	1.7	1.2%
EJY15	780	779.3/390.2*	7.3	5.0%
EJY16	808	807.3/404.2*	4.5	3.0%
EJY17	816	815.3/408.1*	13.1	8.6%
EJY18	852	1702**/851/427*	11.4	7.1%
EJY19	832	831/416*	6.8	4.4%
EJY20	885	885/443*	2.8	1.7%
EJY21	760	1518**/759/380*	22.5	15.7%
EJY22	792	791/396*	8.7	5.8%

*m/2 value ** m·2 value

Table 7: Round 3 Yields. Compound yields and observed MW.

Table 8 displays the hydrophobicity comparison for each compound. Overall, these turned out as expected. EJY19 with the indane side group was the most hydrophobic as predicted, and EJY15, EJY21 and EJY22, with benzyl, furan, and thiophene side chains, respectively, were among the least hydrophobic.

Compound	<i>cLogD</i> _{7.4}	Experimental % ACN
EJY14	-2.36	54.2
EJY15	-2.53	53.5
EJY16	-1.70	55.4
EJY17	-2.24	55.4
EJY18	-0.36	56.2
EJY19	-0.35	57.2
EJY20	-2.37	55.9
EJY21	-4.41	54.1
EJY22	-2.70	54.7

Table 8. Round 3 Hydrophobicity Comparison. Expected versus experimental hydrophobicities.

All Round 3 compounds were tested for activity against *C. neoformans* and toxicity against HepG2 cells. These data, as well as SR values, are listed in **Table 9**. The addition of aromatic moieties proved to increase potency as a whole compared to previous modifications. This can most likely be attributed to an increase in membrane disruption due to the larger, more hydrophobic groups in positions 1 and 4.

One disadvantage of bulkier side chains is the increase in mammalian cytotoxicity. In general, derivatives with the largest groups displayed higher toxicity, such as EJY19 and

EJY20 with the indane and indole residues, respectively. One exception to this was EJY14 with the phenyl moiety. Despite containing a smaller side chain, this compound had increased toxicity against HepG2 cells. This might be explained by the fact that this side chain most closely resembles benzene, which is a known mammalian toxin.⁴² Another explanation for increased toxicity could be due to conformational changes in the molecule since having the phenyl group attached directly to the amide backbone could significantly alter the secondary structure of the peptoid. This would have to be determined through circular dichroism studies. EJY16, EJY17, and EJY22 all produced comparable SRs to RMG8-8. However, none of these quite surpassed the low toxicity of RMG8-8.

Compound	<i>cLogD</i> _{7.4}	<i>C. neoformans</i> MIC (µg/mL)	HepG2 TD ₅₀ (µg/mL)	Selectivity Ratio
RMG8-8	-2.38	1.56-3.13	175	56
EJY14	-2.36	1.56-3.13	81 ± 33	26
EJY15	-2.53	1.56-3.13	145 ± 40	46
EJY16	-1.70	1.56-3.13	167 ± 12	53
EJY17	-2.24	1.56-3.13	150 ± 33	48
EJY18	-0.36	6.25	118 ± 52	19
EJY19	-0.35	1.56-3.13	91 ± 1	29
EJY20	-2.37	1.56-3.13	85 ± 43	27
EJY21	-4.41	3.13-6.25	143 ± 16	23
EJY22	-2.70	1.56-3.13	154 ± 10	49

Table 9. Round 3 MIC and TD₅₀ Data. Efficacy of Round 3 derivatives compared to RMG8-8.

Hemolytic Activity

Since none of the SAR derivatives were more potent and less toxic than RMG8-8 based on the above testing, it was decided that hemolytic testing would be a valuable comparator to make. Hemolysis is the breakdown or lysis of red blood cells (RBCs), so this data is an additional facet of toxicity.³⁵ Hemolysis of RBCs is an undesired outcome of any antimicrobial treatment because RBCs are responsible for oxygen transport in the body via the protein hemoglobin. While mammalian cytotoxicity and hemolytic activity are often similar, this is not always the case. This is likely due to the different mechanisms of action.⁴³ Cytotoxicity is localized to organs involved in molecule metabolism, whereas hemolysis affects RBCs which circulate throughout the body.

The top performing derivatives from Rounds 2 and 3 were selected for hemolytic testing: EJY9, EJY16, EJY17, and EJY22. Because hemolysis can be donor specific, it was important to test RMG8-8 along with the selected derivatives against the same sample of human RBCs. **Table 10** shows HC_{10} values which is the concentration of peptoid that causes lysis of 10% of the RBCs. EJY9 ($HC_{10} = 130 \pm 45 \mu\text{g/mL}$) showed promising results as it was significantly less hemolytic than RMG8-8 ($HC_{10} = 75 \pm 31 \mu\text{g/mL}$). EJY22 displayed comparable hemolytic activity, and EJY16 and EJY17 were determined to be more hemolytic than RMG8-8. The decrease in hemolysis between EJY9 and RMG8-8 is most likely attributed to the less bulky isobutyl residues on EJY9 and overall decrease in hydrophobicity of this compound compared to the cyclohexyl side chains on RMG8-8. It is also interesting to note that there is a direct correlation between hydrophobicity and hemolytic activity. This certainly contributes to the decreased hemolytic activity of EJY9 even though this compound had similar mammalian cytotoxicity to RMG8-8.

Compound	<i>cLogD</i> _{7.4}	HC ₁₀ ($\mu\text{g}/\text{mL}$)
RMG8-8	-2.38	75 \pm 31
EJY9	-3.49	130 \pm 45
EJY16	-1.70	38 \pm 11
EJY17	-2.24	59 \pm 22
EJY22	-2.70	81 \pm 37

Table 10. HC₁₀ Values. Hemolytic activity for selected derivatives compared to RMG8-8.

CHAPTER 4: CONCLUSIONS

The goal of this research was to optimize a lead antifungal peptoid, RMG8-8, via an SAR study. We hypothesized that through submonomer modification we could improve the overall activity and selectivity of this compound. A 3-round SAR was executed, with each round utilizing a different strategy of modification. Round 1 consisted of lipophilic tail derivatives in position 5 and other miscellaneous alterations. Round 2 included varying aliphatic residues in positions 1 and 4. Round 3 contained aromatic derivatives in positions 1 and 4. Round 1 compounds were tested against *C. albicans* and *C. neoformans* while Rounds 1 and 2 were tested only against *C. neoformans*, making that the main priority of the study. While no single derivative was improved across all data points, there were improvements made on hemolytic activity with EJY9. For this same compound, the MIC against *C. neoformans* and HepG2 cytotoxicity were comparable to those of RMG8-8. EJY9 could be an important compound to further evaluate given its promising data thus far.

Another plan for future research is to modify the fluorinated benzene derivative (EJY17) to assess the effects of the other halogens on compound efficacy. Previous studies have indicated that changes in halogenation on phenyl side chains can modulate peptoid potency and toxicity.⁴⁰ Perhaps another halogenated derivative will display decreased hemolytic activity, opening the door to other potential derivatives with favorable activity. It might also be worthwhile to investigate the properties of EJY5 and EJY7 since they had increased potency against *C. albicans* compared to RMG8-8. The scrambled monomer positioning of EJY7 and chiral side chains of EJY16 seemed to have an overall positive effect on activity, making these ideal candidates for future exploration.

References

1. Lockhart, S. R. Current Epidemiology of Candida Infection. *Clin. Microbiol. Newsl.* **36**, 131–136 (2014).
2. Tande, A. J. & Patel, R. Prosthetic joint infection. *Clin. Microbiol. Rev.* **27**, 302–345 (2014).
3. Hirano, R., Sakamoto, Y., Kudo, K. & Ohnishi, M. Retrospective analysis of mortality and Candida isolates of 75 patients with candidemia: A single hospital experience. *Infect. Drug Resist.* **8**, 199–205 (2015).
4. Mayer, F. L., Wilson, D. & Hube, B. Candida albicans pathogenicity mechanisms. *Virulence* **4**, 119–128 (2013).
5. Nobile, C. J. & Johnson, A. D. Candida albicans Biofilms and Human Disease. *Annu. Rev. Microbiol.* **69**, 71–92 (2015).
6. Manley, G. How Sweet it is! Cell Wall Biogenesis and Polysaccharide Capsule Formation in *Cryptococcus neoformans*. *Annu. Rev. Microbiol.* **63**, 233–247 (2013).
7. Buchanan, K. L. & Murphy, J. W. What makes *Cryptococcus neoformans* a pathogen? *Emerg. Infect. Dis.* **4**, 71–83 (1998).
8. Sloan, D. J. & Parris, V. Cryptococcal meningitis: epidemiology and therapeutic options. *Clin. Epidemiol.* **6**, 169–182 (2014).
9. Park, B. J. *et al.* Estimation of the current global burden of cryptococcal meningitis among persons living with HIV/AIDS. *AIDS* **23**, (2009).
10. Rajasingham, R. Global burden of disease of HIV-associated cryptococcal meningitis: an updated analysis. *Physiol. Behav.* **176**, 139–148 (2017).
11. Merry, M. & Boulware, D. R. Clinical Infectious Diseases Cryptococcal Meningitis Treatment Strategies Affected by the Explosive Cost of Flucytosine in the United States: A Cost-effectiveness Analysis. (2016). doi:10.1093/cid/ciw151
12. Datta, K. *et al.* Spread of *Cryptococcus gattii* into Pacific Northwest Region of the United States. *Emerg. Infect. Dis.* **15**, 1185 (2009).
13. Chen, S. C. A., Meyer, W. & Sorrell, T. C. *Cryptococcus gattii* infections. *Clin. Microbiol. Rev.* **27**, 980–1024 (2014).
14. Segal, E. & Elad, D. Special issue: Treatments for fungal infections. *J. Fungi* **4**, 10–12 (2018).
15. Perfect, J. R. *et al.* Guideline for cryptococcus. *Clin Infect Dis* **50**, 291–322 (2018).
16. Pappas, P. G. *et al.* 2009 Update by the Infectious Diseases Society of America. **48**, 503–535 (2009).

17. Mesa-Arango, A. C., Scorzoni, L. & Zaragoza, O. It only takes one to do many jobs: Amphotericin B as antifungal and immunomodulatory drug. *Front. Microbiol.* **3**, 1–10 (2012).
18. Kanafani, Z. A. & Perfect, J. R. Resistance to antifungal agents: Mechanisms and clinical impact. *Clin. Infect. Dis.* **46**, 120–128 (2008).
19. Vermes, A., Guchelaar, H. J. & Dankert, J. Flucytosine: A review of its pharmacology, clinical indications, pharmacokinetics, toxicity and drug interactions. *J. Antimicrob. Chemother.* **46**, 171–179 (2000).
20. Ben-Ami, R. & Kontoyiannis, D. P. Resistance to Antifungal Drugs. *Infect. Dis. Clin. North Am.* **35**, 279–311 (2021).
21. Zafar, H., Altamirano, S., Ballou, E. R. & Nielsen, K. A titanic drug resistance threat in *Cryptococcus neoformans*. *Curr. Opin. Microbiol.* **52**, 158–164 (2019).
22. Nakatsuji, T. & Gallo, R. L. Antimicrobial peptides: Old Molecules with New Ideas. *J. Invest. Dermatol.* **132**, 887–895 (2012).
23. Matejuk, A. *et al.* Peptide-based antifungal therapies against emerging infections. *Drugs Future* **35**, 197–217 (2010).
24. Green, R. M. & Bicker, K. L. Evaluation of Peptoid Mimics of Short, Lipophilic Peptide Antimicrobials. *Int. J. Antimicrob. Agents* **56**, 106048 (2020).
25. Chongsiriwatana, N. P. *et al.* Peptoids that mimic the structure, function, and mechanism of helical antimicrobial peptides. *Proc. Natl. Acad. Sci. USA* **105**, 2794 (2008).
26. Gomes Von Borowski, R., Gnoatto, S. C. B., Macedo, A. J. & Gillet, R. Promising Antibiofilm Activity of Peptidomimetics. *Frontiers in Microbiology* **9**, 2157 (2018).
27. Mroz, P. A., Perez-Tilve, D., Mayer, J. P. & DiMarchi, R. D. Stereochemical inversion as a route to improved biophysical properties of therapeutic peptides exemplified by glucagon. *Commun. Chem.* **2**, 1–8 (2019).
28. Evans, B. J., King, A. T., Katsifis, A., Matesic, L. & Jamie, J. F. Methods to enhance the metabolic stability of peptide-based PET radiopharmaceuticals. *Molecules* **25**, (2020).
29. Mojsoska, B., Zuckermann, R. N. & Jenssen, H. Structure-Activity Relationship Study of Novel Peptoids That Mimic the Structure of Antimicrobial Peptides. *Antimicrob. Agents Chemother.* **59**, 4112–4120 (2015).
30. Corson, A. E., Armstrong, S. A., Wright, M. E., McClelland, E. E. & Bicker, K. L. Discovery and Characterization of a Peptoid with Antifungal Activity against *Cryptococcus neoformans*. *ACS Med. Chem. Lett.* **7**, 1139–1144 (2016).

31. Zuckermann, R. N., Kerr, J. M., Kent, S. B. H. & Moosf, W. H. Efficient Method for the Preparation of Peptoids. 10646–10647 (1992).
32. Tran, H., Gael, S. L., Connolly, M. D. & Zuckermann, R. N. Solid-phase submonomer synthesis of peptoid polymers and their self-assembly into highly-ordered nanosheets. *J. Vis. Exp.* 1–7 (2011). doi:10.3791/3373
33. Patch, J. A. & Barron, A. E. Helical Peptoid Mimics of Magainin-2 Amide. *J. Am. Chem. Soc.* **125**, 12092–12093 (2003).
34. Middleton, M. P., Armstrong, S. A. & Bicker, K. L. Improved Potency and Reduced Toxicity of the Antifungal Peptoid AEC5 Through Submonomer Modification. *Bioorg. Med. Chem. Lett.* **28**, 3514–3519 (2018).
35. Green, R. M. & Bicker, K. L. Discovery and Characterization of a Rapidly Fungicidal and Minimally Toxic Peptoid against *Cryptococcus neoformans*. (2021). doi:10.1021/acsmchemlett.1c00327
36. Bicker, K. L. & Cobb, S. L. Recent advances in the development of anti-infective peptoids. *Chem. Commun.* **56**, 11158–11168 (2020).
37. Luo, Y. *et al.* Peptoid Efficacy against Polymicrobial Biofilms Determined by Using Propidium Monoazide-Modified Quantitative PCR. *ChemBioChem* **18**, 111–118 (2017).
38. Fisher, K. J., Turkett, J. A., Corson, A. E. & Bicker, K. L. Peptoid Library Agar Diffusion (PLAD) Assay for the High-Throughput Identification of Antimicrobial Peptoids. *ACS Comb. Sci.* **18**, 287–291 (2016).
39. CLSI. *Reference Method for Broth Dilution Antifungal Susceptibility Testing of Yeasts; Approved Standard-Third Edition; CLSI Document M27-A3.*; Clinical and Laboratory Standards Institute: Wayne, PA, PA, (2008).
40. Molchanova, N. *et al.* Halogenation as a tool to tune antimicrobial activity of peptoids. *Sci. Rep.* **10**, 14805 (2020).
41. Mishra, N. *et al.* Efficient hepatic delivery of drugs: Novel strategies and their significance. *Biomed Res. Int.* **2013**, (2013).
42. Medinsky, M. A., Schlosser, P. M. & Bond, J. A. Critical issues in benzene toxicity and metabolism: The effect of interactions with other organic chemicals on risk assessment. *Environ. Health Perspect.* **102**, 119–124 (1994).
43. Wang, Y. *et al.* Exploration of the correlation between the structure, hemolytic activity, and cytotoxicity of steroid saponins. *Bioorganic Med. Chem.* **15**, 2528–2532 (2007).

APPENDIX

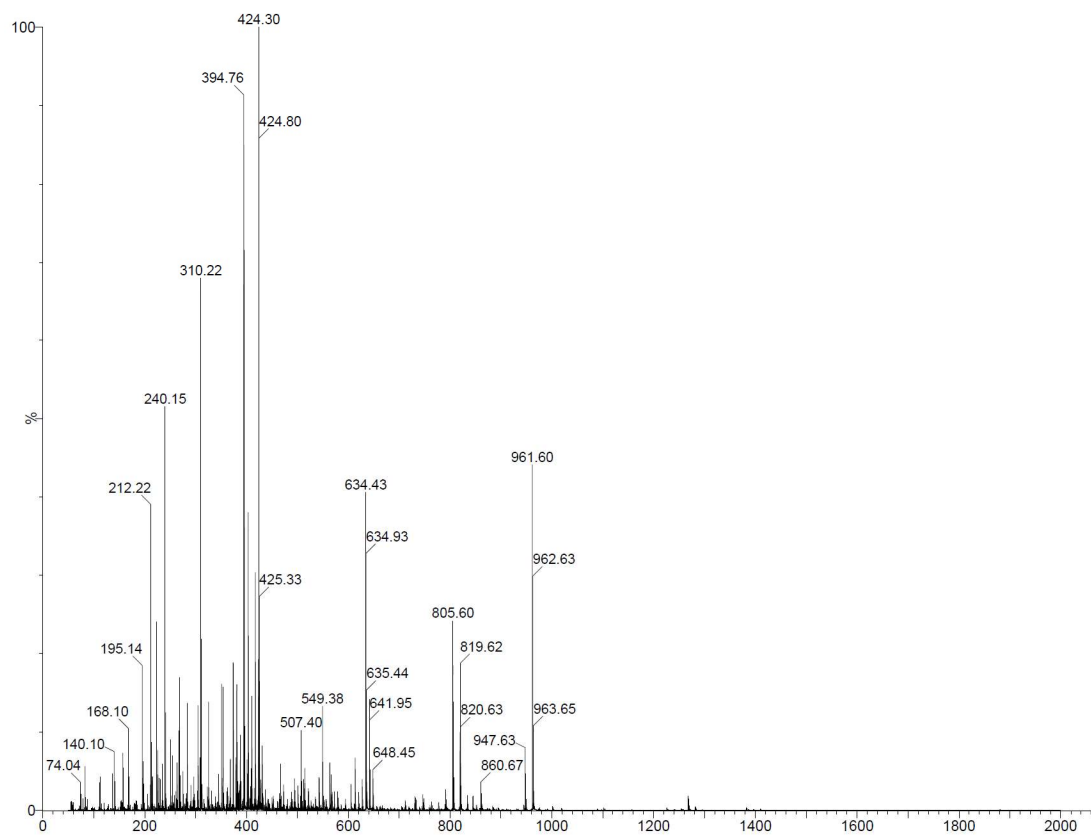


Figure 12. Mass spectra of EJY1 confirming expected mass of 849 g/mol, which shows up at 424 m/z ($849/2$).

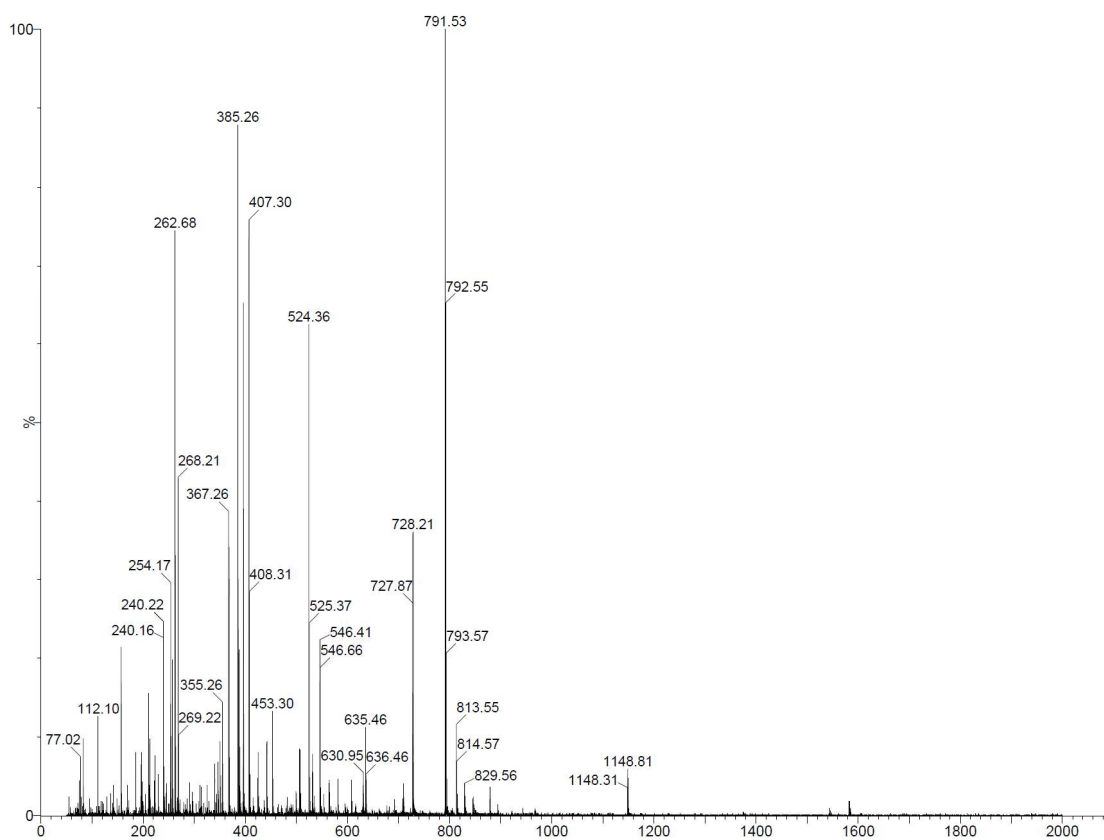


Figure 13. Mass spectra of EJY2 confirming expected mass of 792 g/mol.

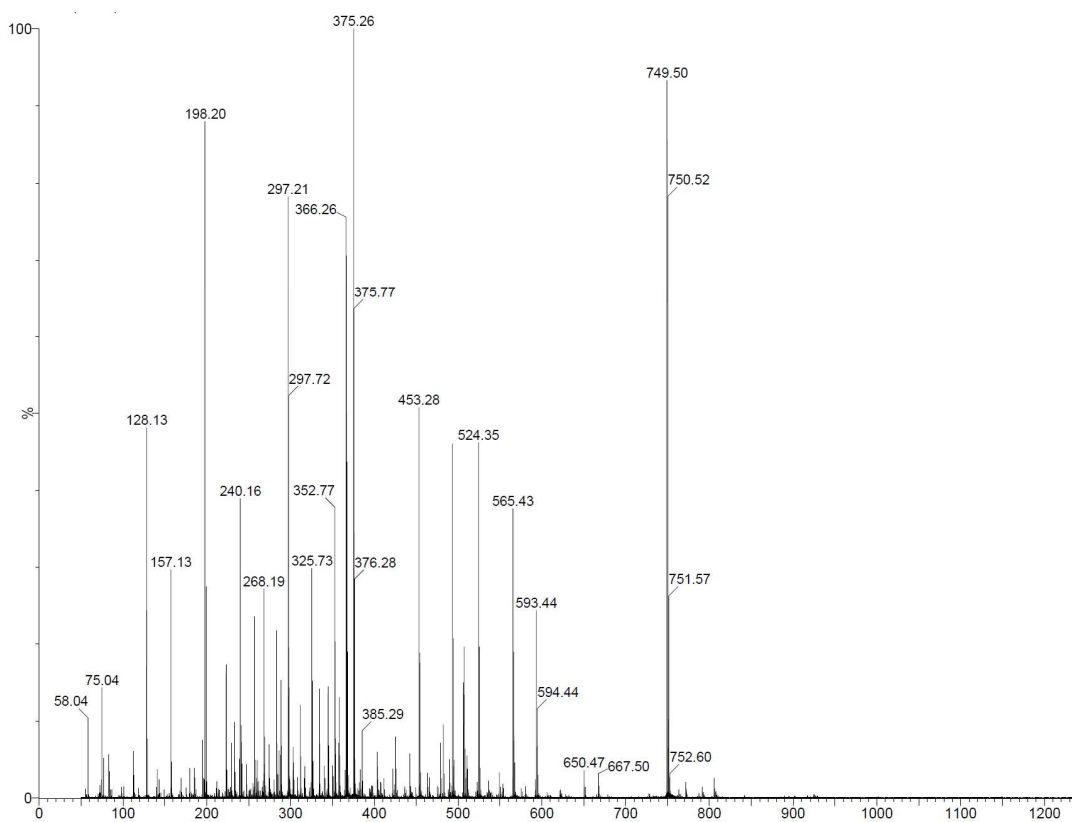


Figure 14. Mass spectra of EJY3 confirming expected mass of 750 g/mol.

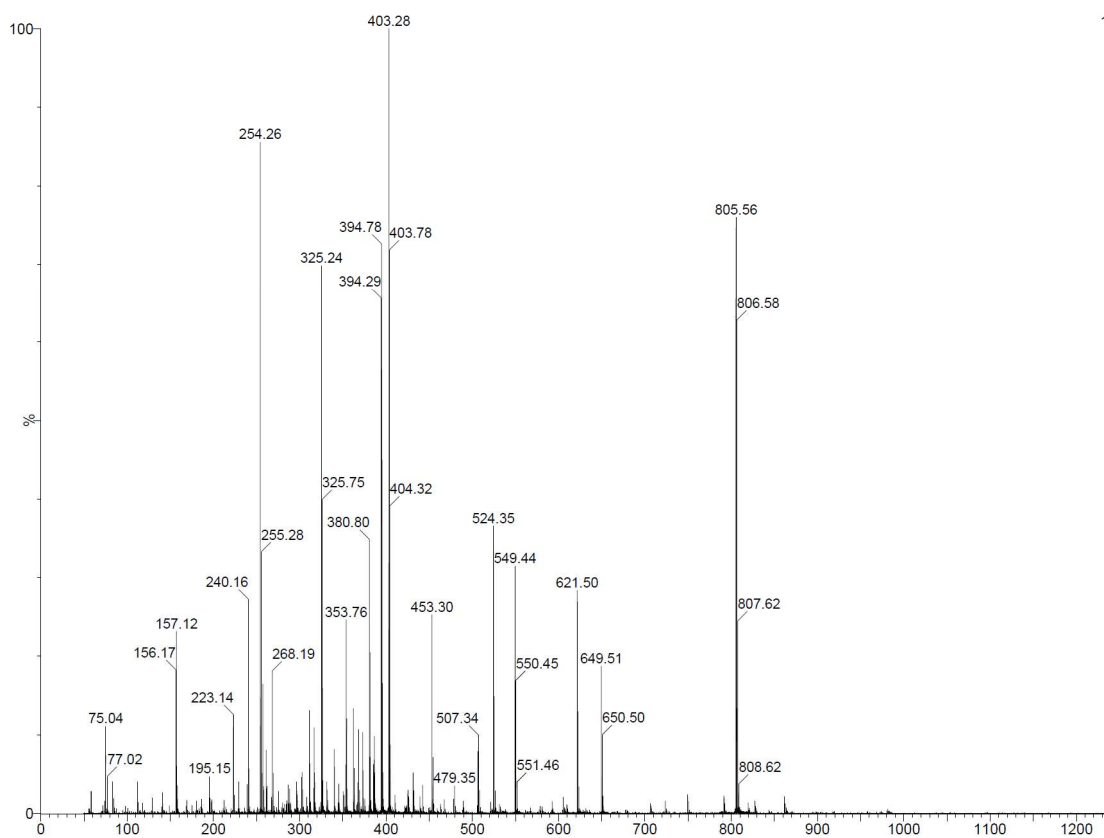


Figure 15. Mass spectra of EJY4 confirming expected mass of 806 g/mol.

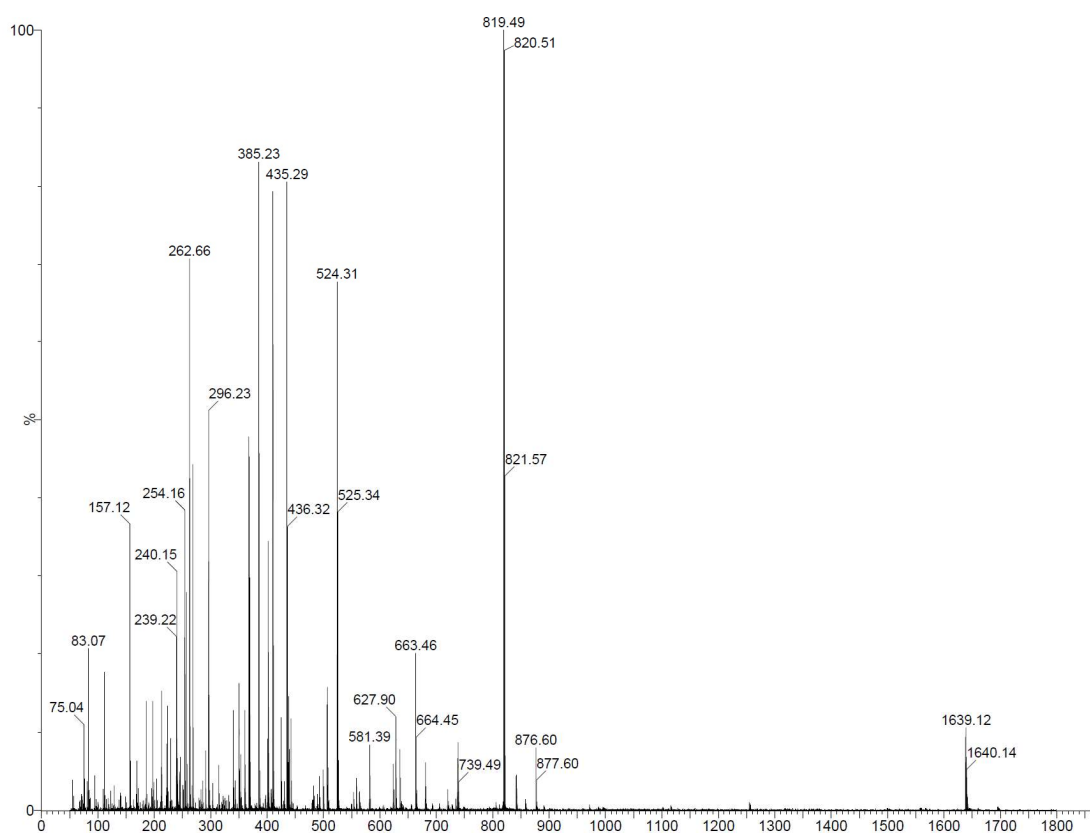


Figure 16. Mass spectra of EJY5 confirming expected mass of 820 g/mol.

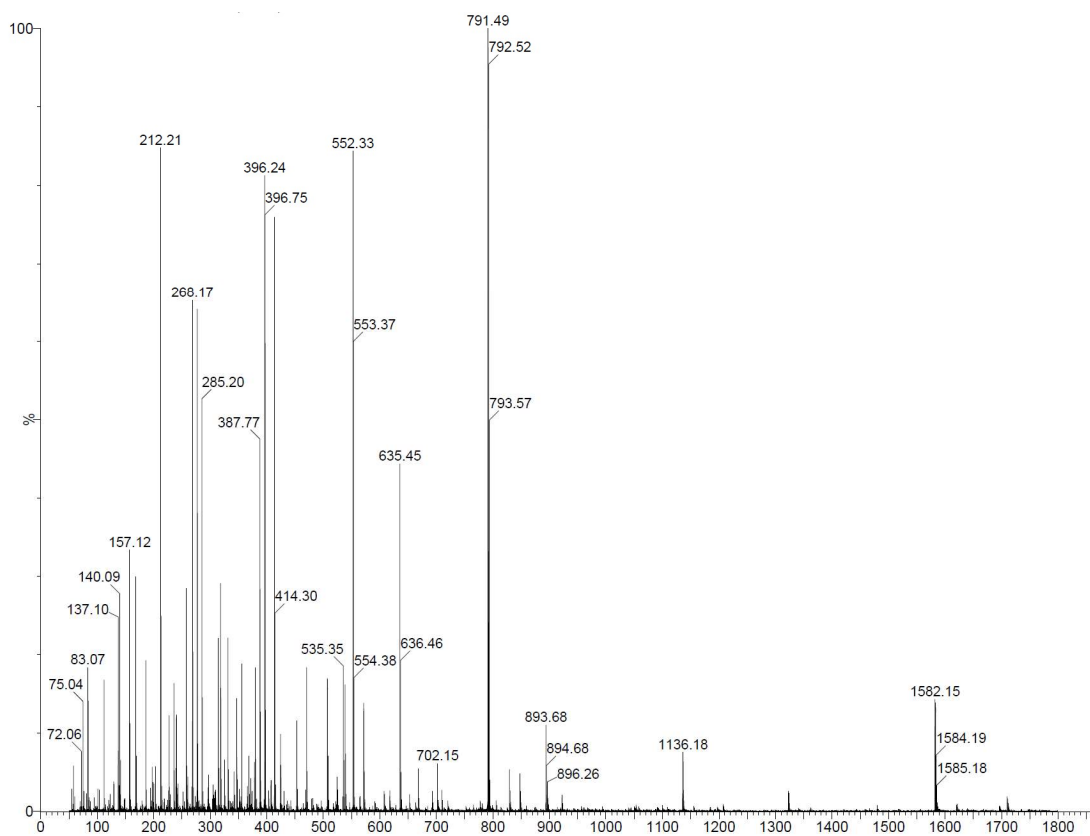


Figure 17. Mass spectra of EJY6 confirming expected mass of 792 g/mol.

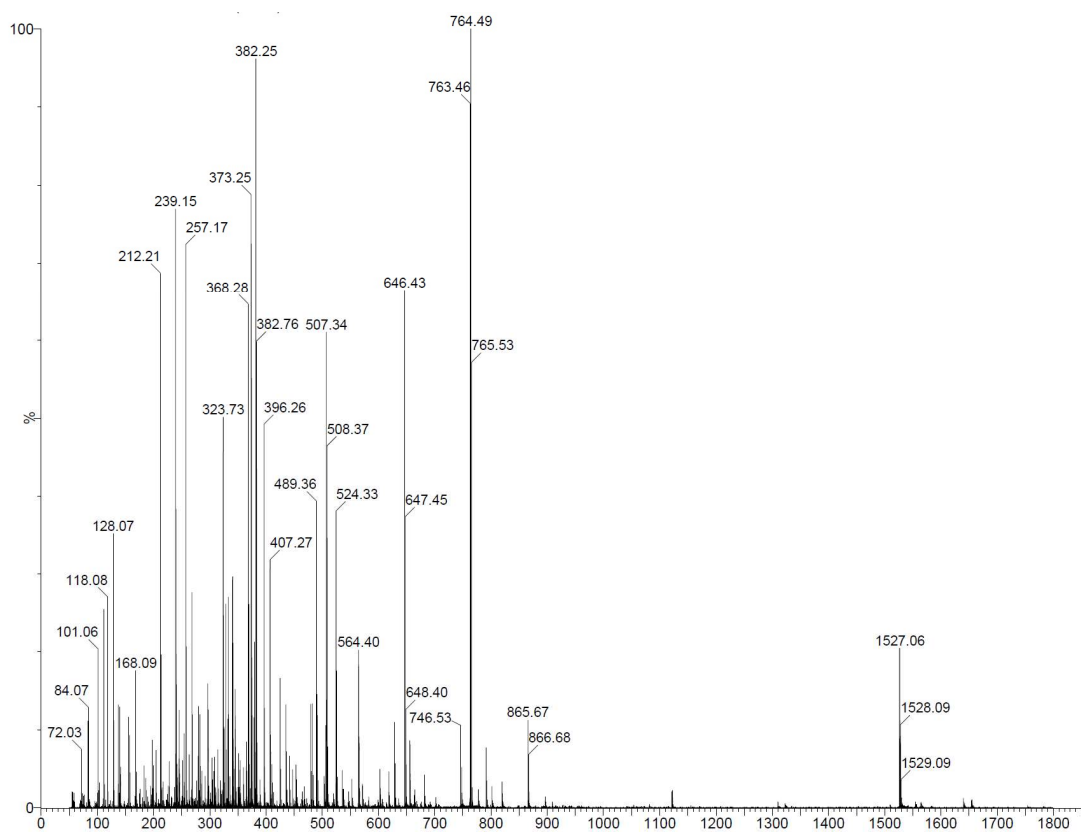


Figure 18. Mass spectra of EJY7 confirming expected mass of 764 g/mol.

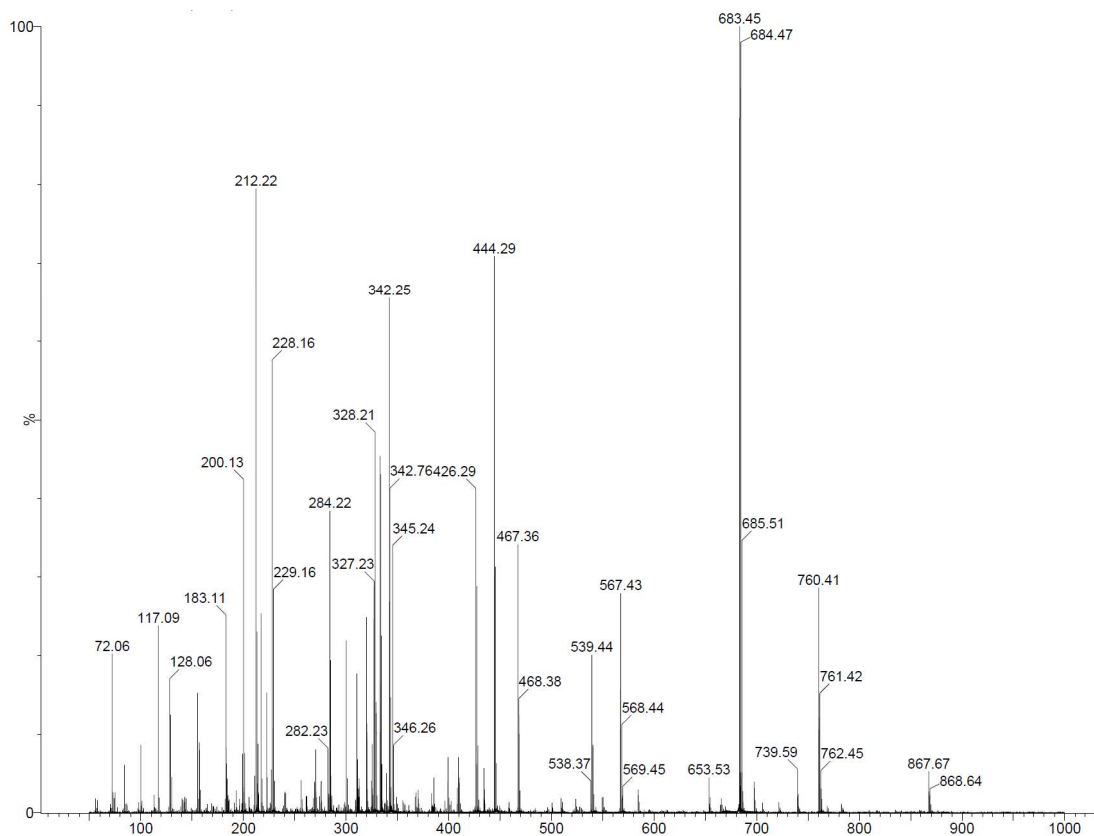


Figure 19. Mass spectra of EJY8 confirming expected mass of 684 g/mol.

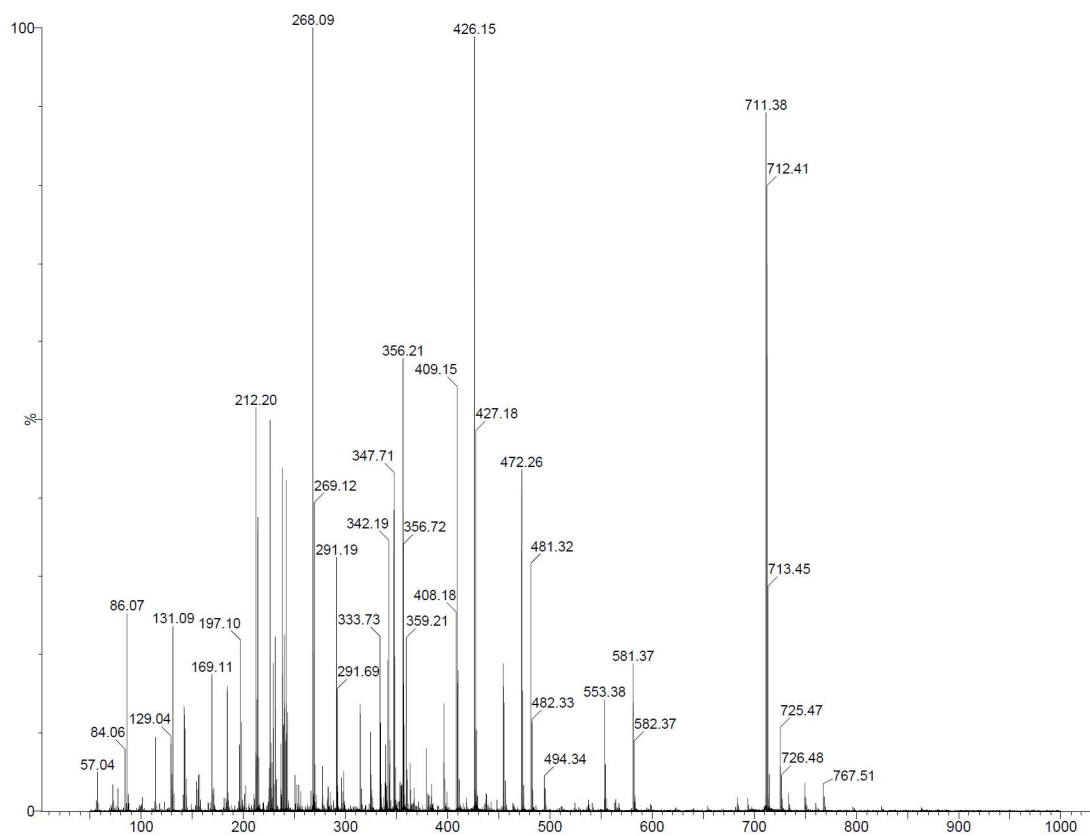


Figure 20. Mass spectra of EJY9 confirming expected mass of 712 g/mol.

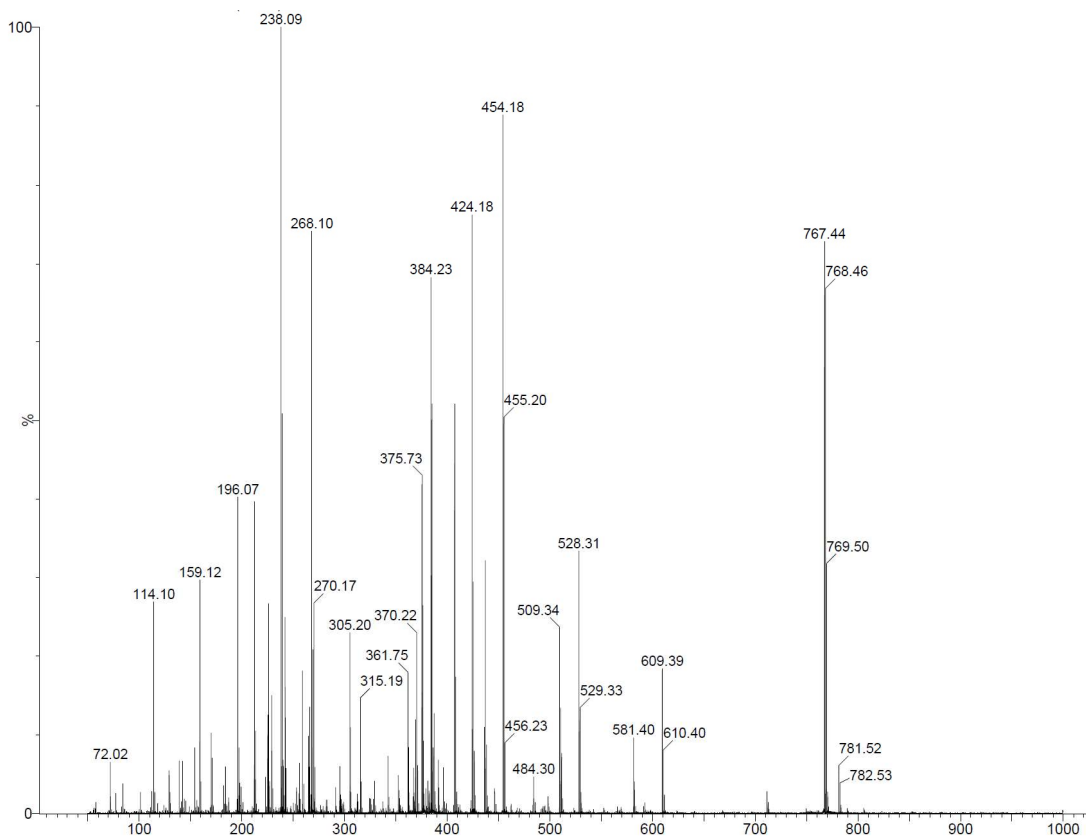


Figure 21. Mass spectra of EJY10 confirming expected mass of 768 g/mol.

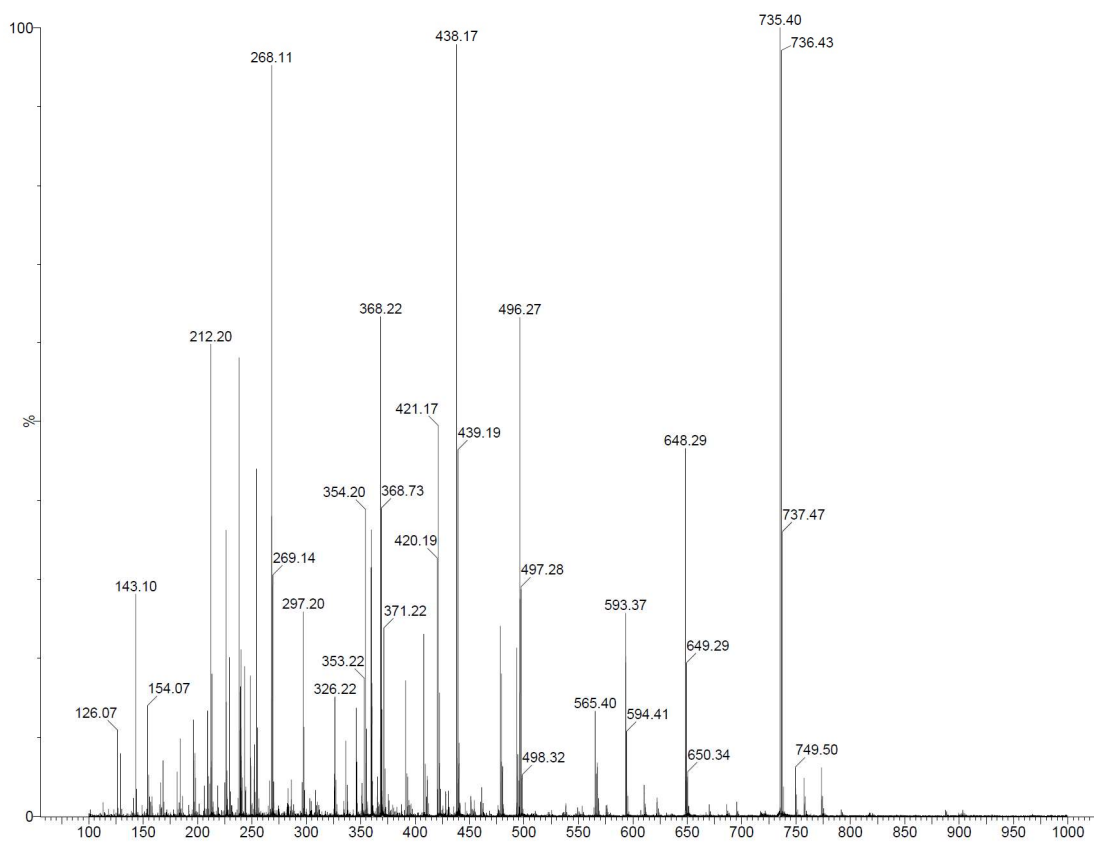


Figure 22. Mass spectra of EJY11 confirming expected mass of 736 g/mol.

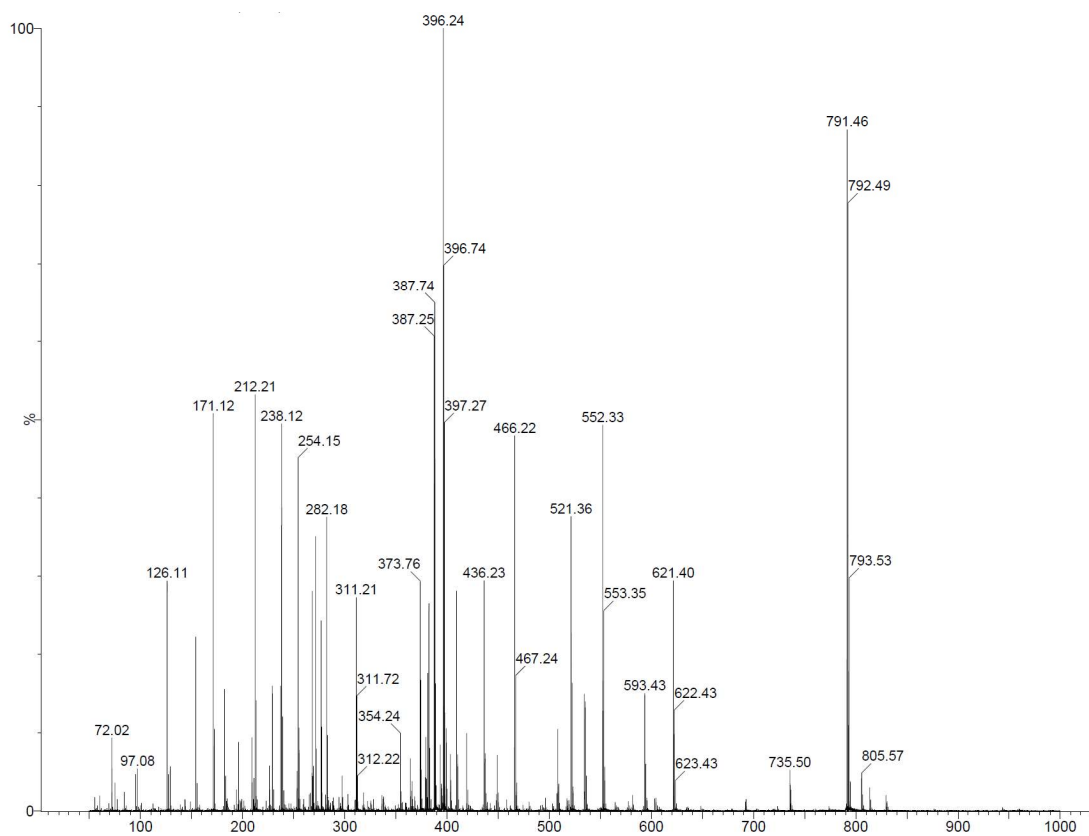


Figure 23. Mass spectra of EJY12 confirming expected mass of 792 g/mol.

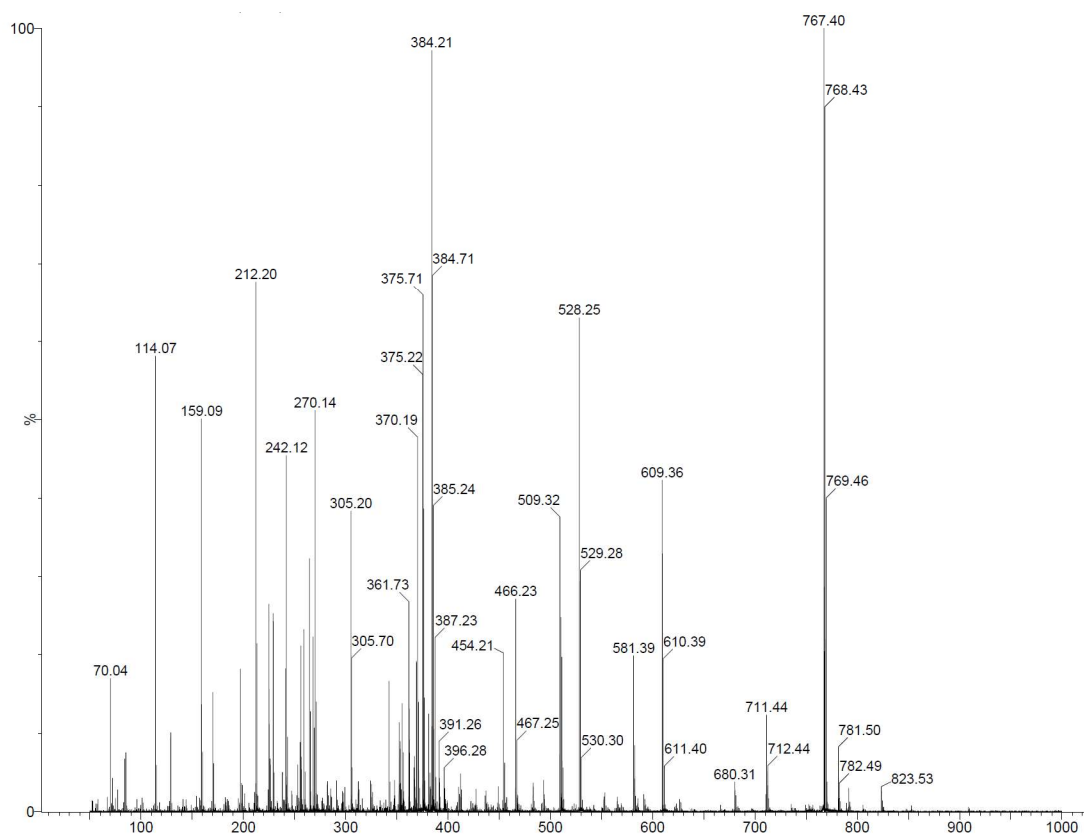


Figure 24. Mass spectra of EJY13 confirming expected mass of 768 g/mol.

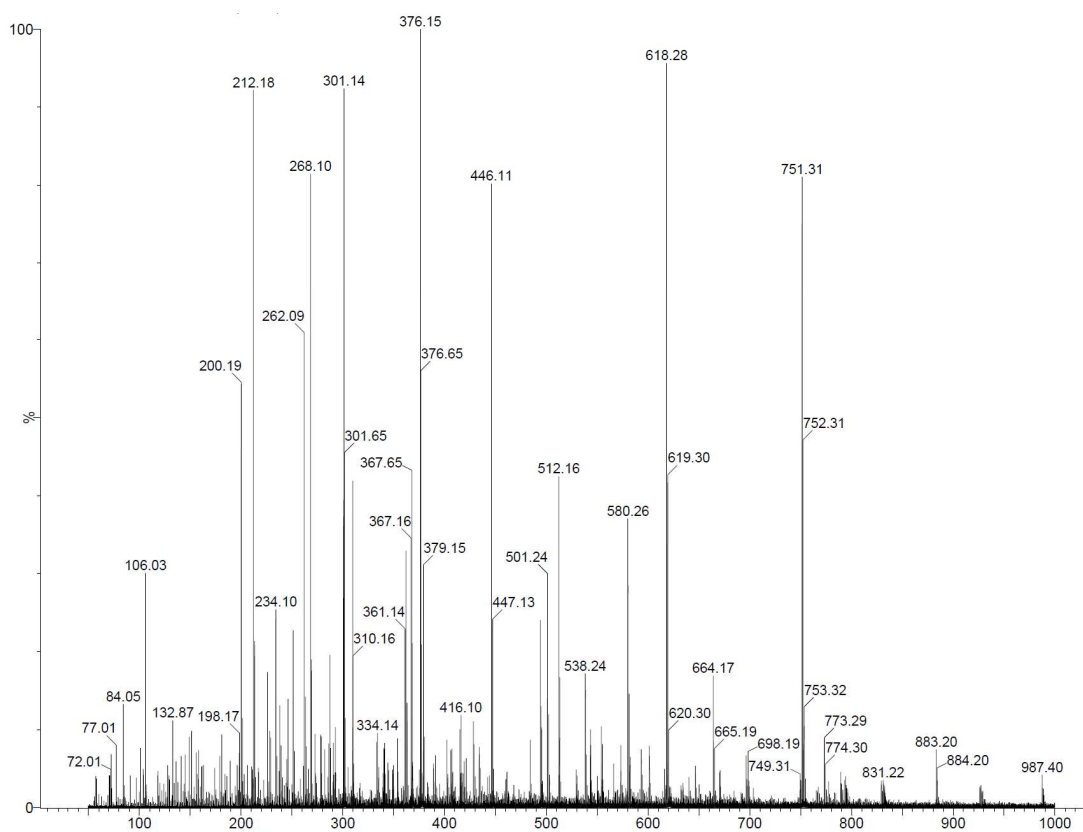


Figure 25. Mass spectra of EJY14 confirming expected mass of 752 g/mol.

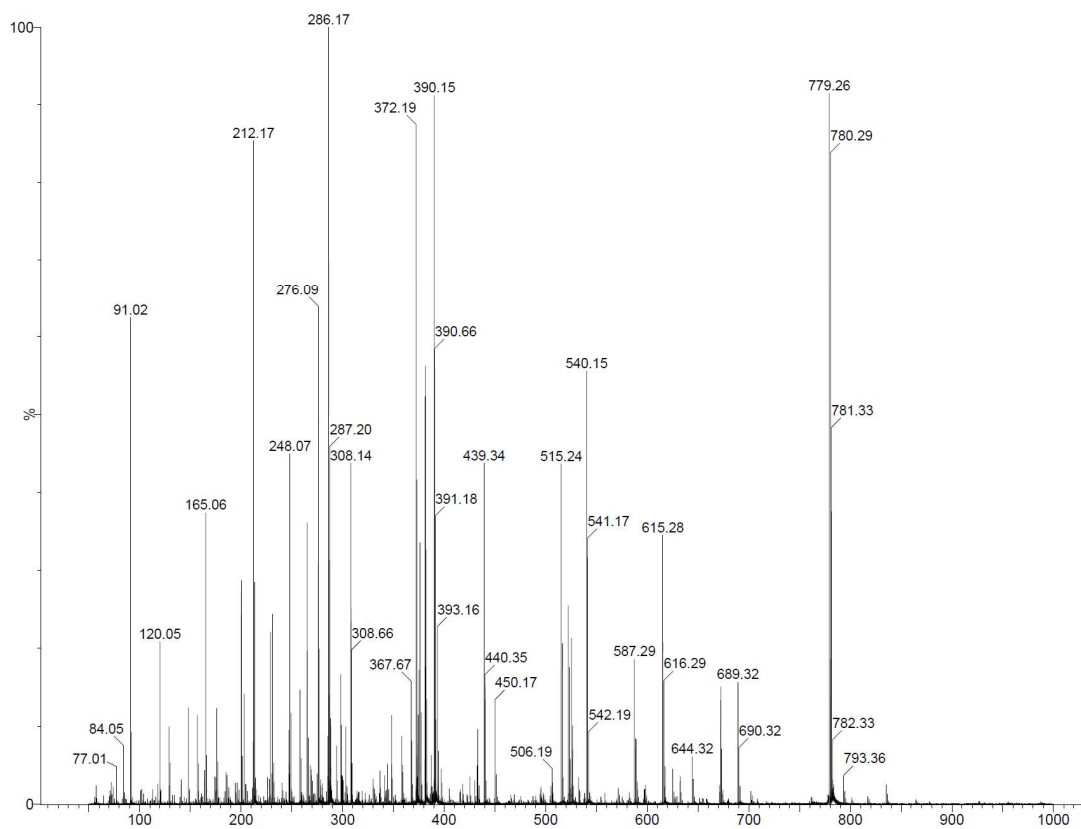


Figure 26. Mass spectra of EJY15 confirming expected mass of 780 g/mol.

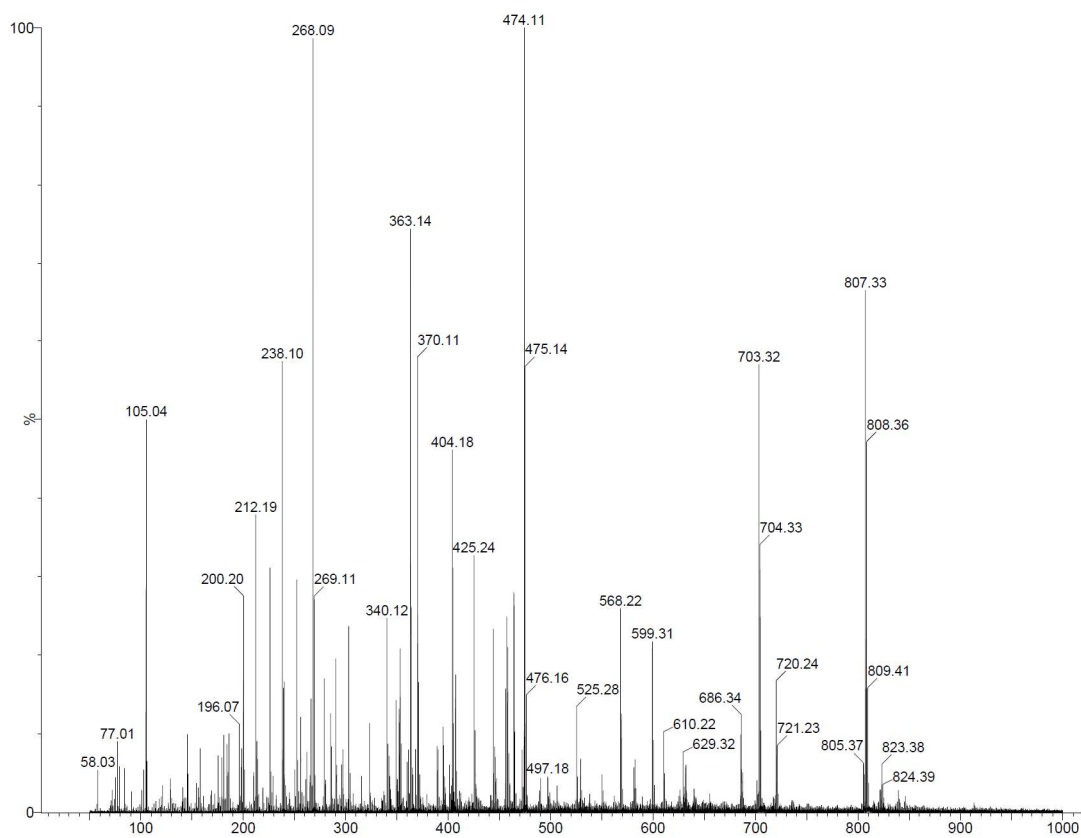


Figure 27. Mass spectra of EJY16 confirming expected mass of 808 g/mol.

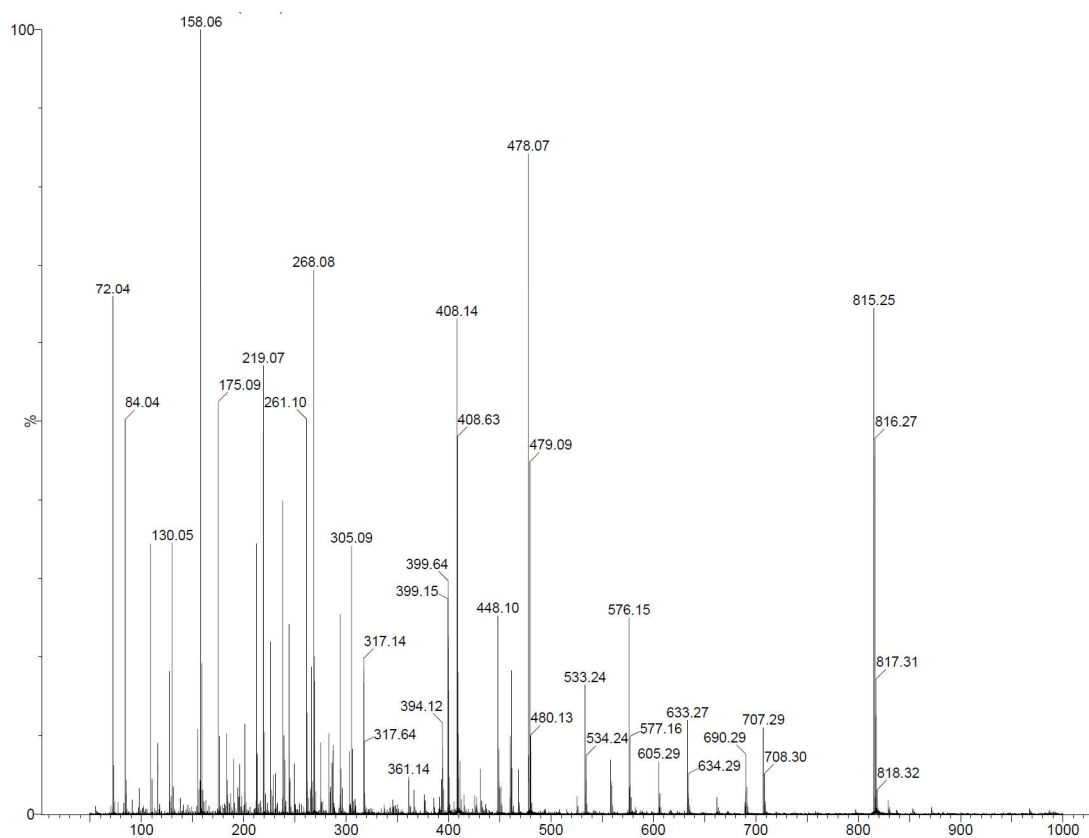


Figure 28. Mass spectra of EJY17 confirming expected mass of 816 g/mol.

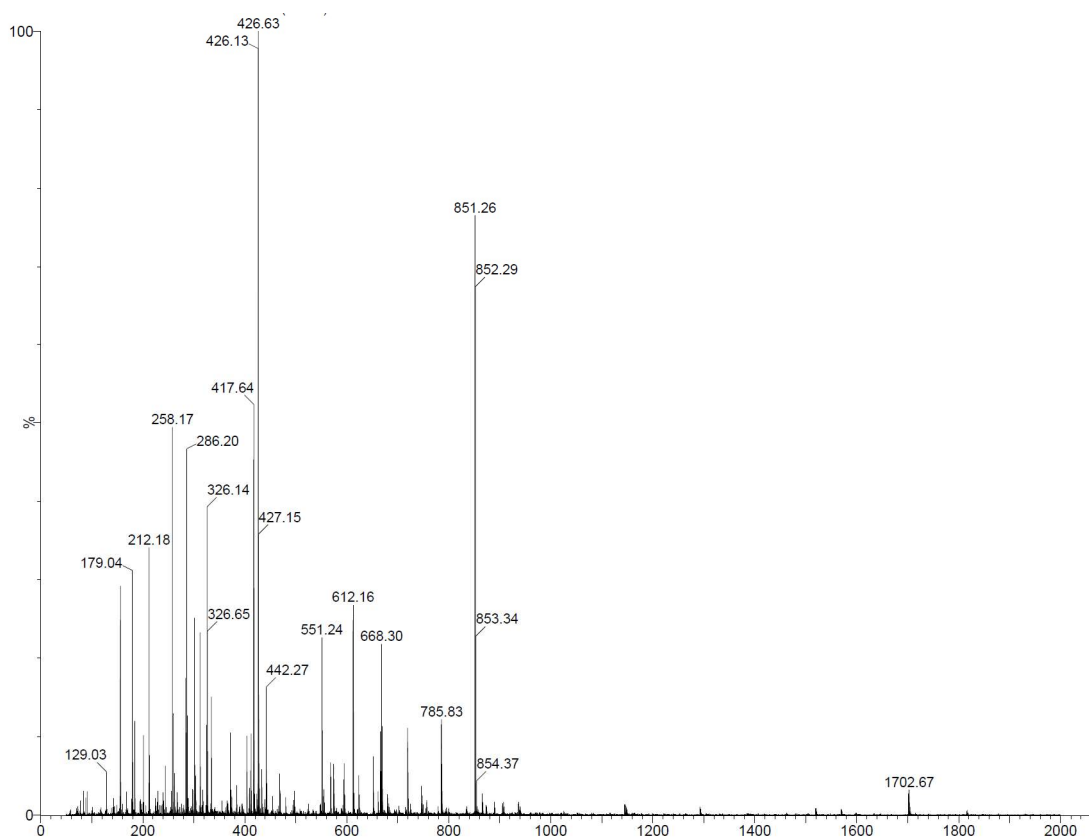


Figure 29. Mass spectra of EJY18 confirming expected mass of 852 g/mol.

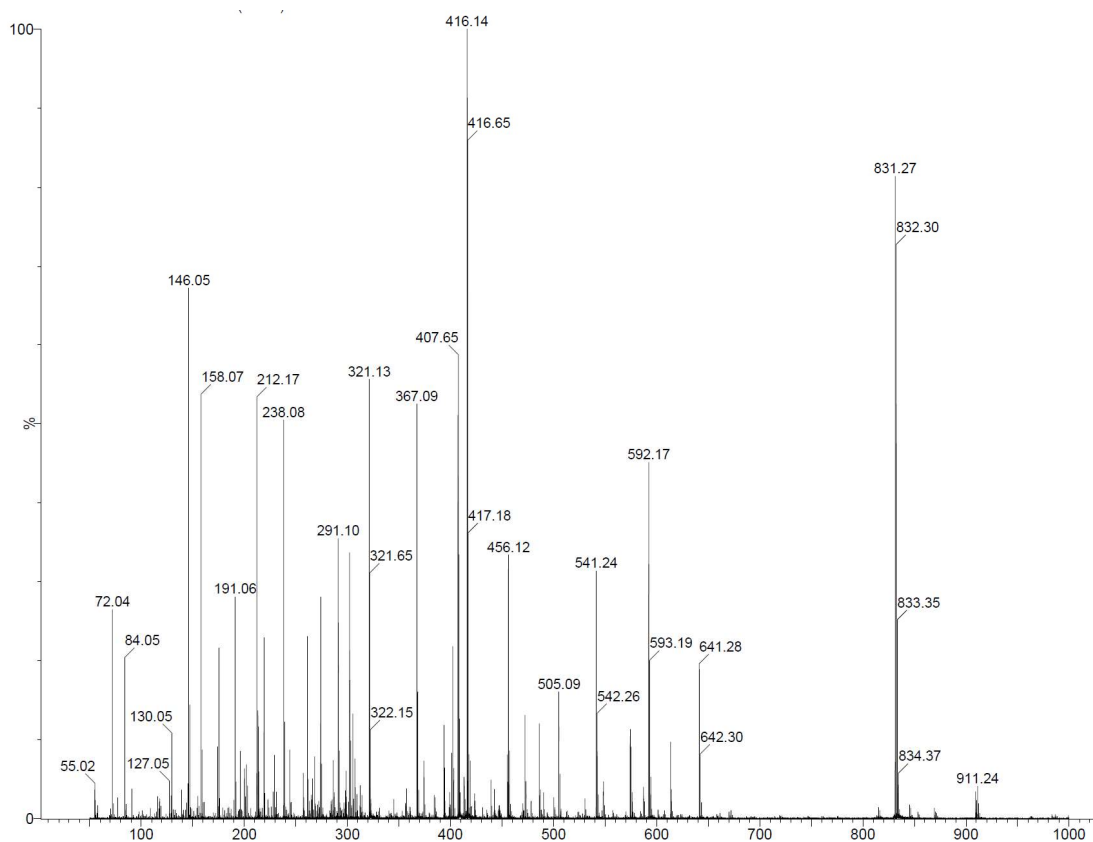


Figure 30. Mass spectra of EJY19 confirming expected mass of 832 g/mol.

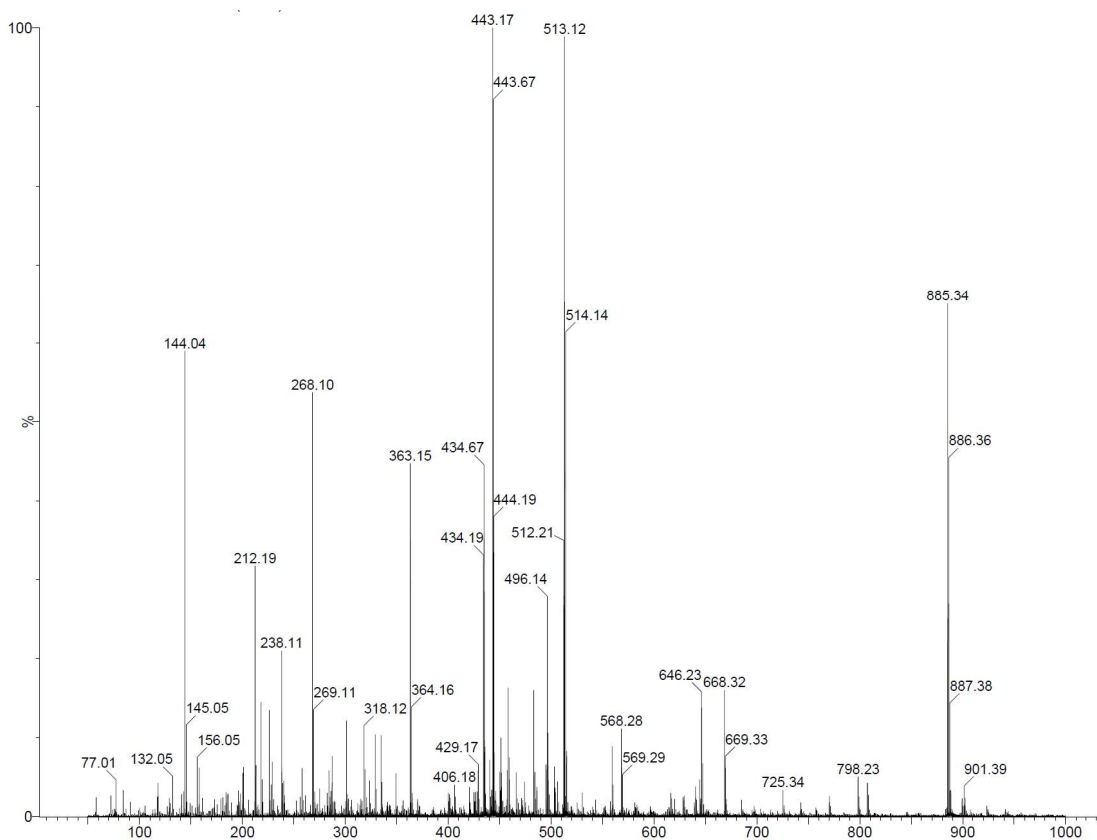


Figure 31. Mass spectra of EJY20 confirming expected mass of 885 g/mol.

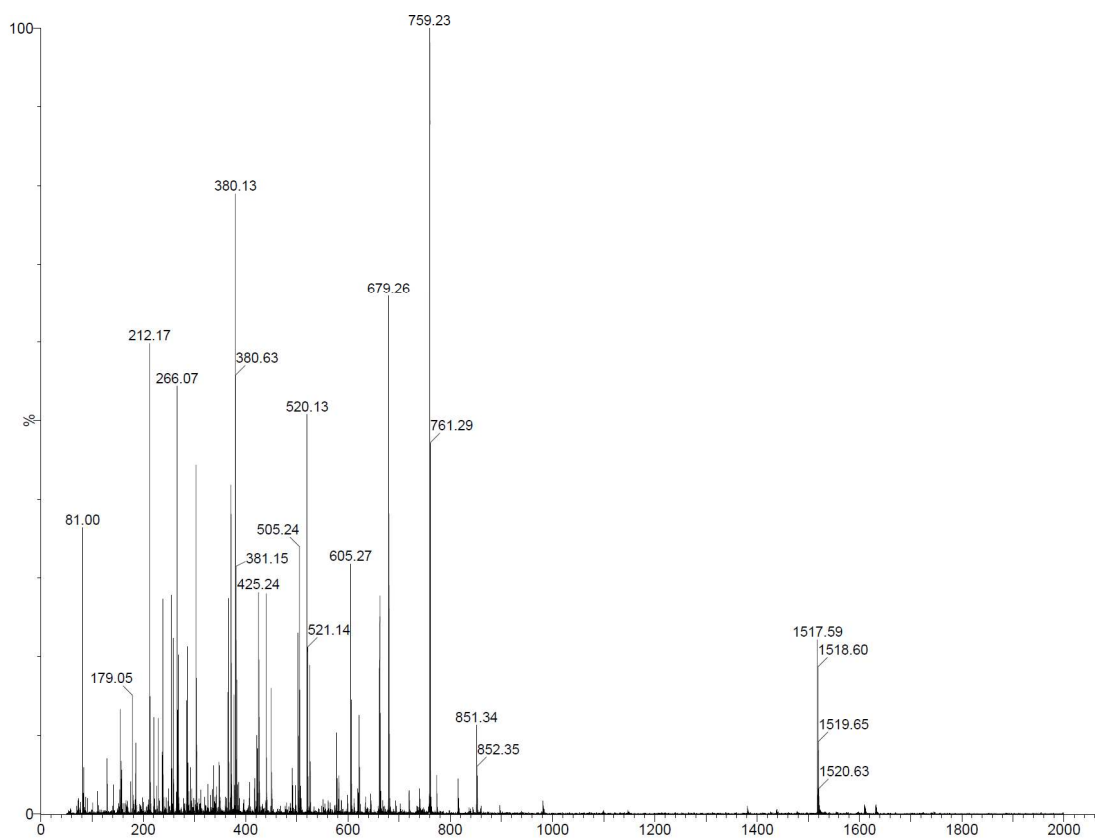


Figure 32. Mass spectra of EJY21 confirming expected mass of 760 g/mol.

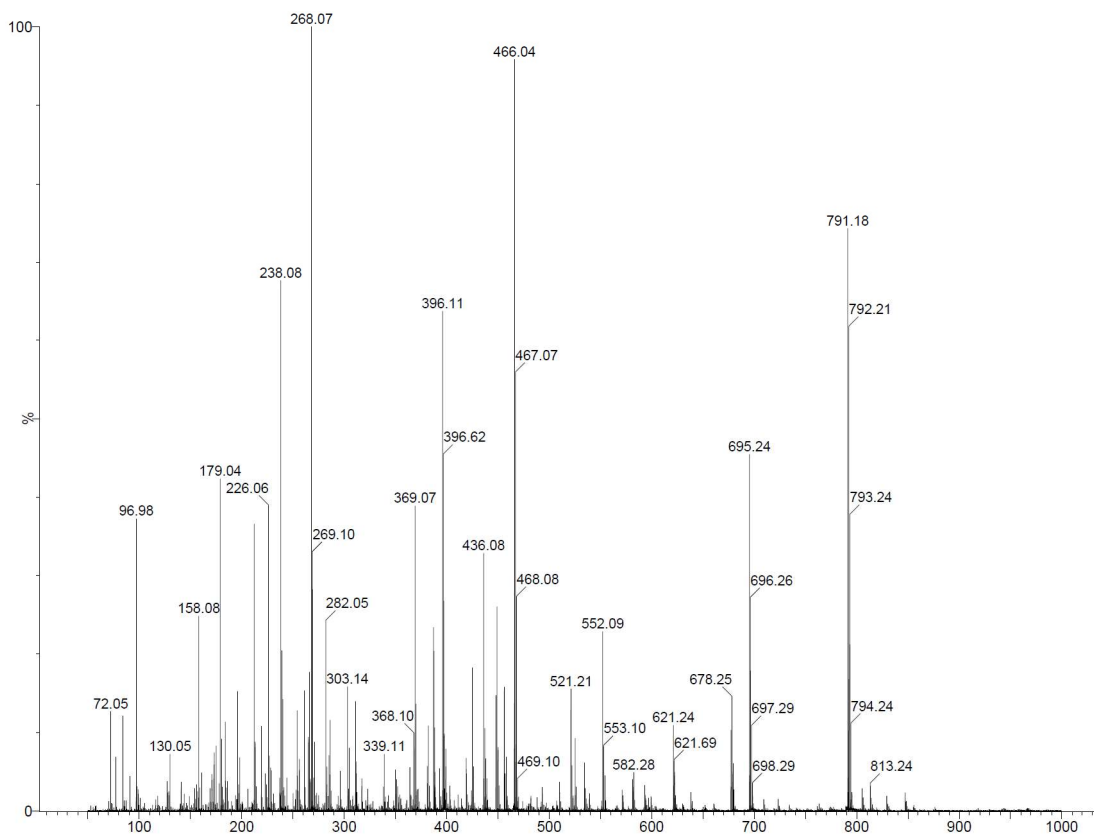


Figure 33. Mass spectra of EJY22 confirming expected mass of 792 g/mol.